J|A|C|S
ARTICLES
Published on Web 06/19/2007

Time-Domain *ab Initio* Study of Charge Relaxation and Recombination in Dye-Sensitized TiO_2

Walter R. Duncan, Colleen F. Craig, and Oleg V. Prezhdo*

Contribution from the Department of Chemistry, University of Washington, Seattle, Washington 98195-1700

Received January 31, 2007; E-mail: prezhdo@u.washington.edu

Abstract: In order to investigate the electron dynamics at the alizarin/I_2^-/TiO_2 interface this study uses a novel state-of-the-art quantum-classical approach that combines time-dependent density functional theory with surface hopping in the Kohn−Sham basis. Representing the dye-sensitized semiconductor Grätzel cell with the I^-/I_3^- mediator, the system addresses the problems of an organic/inorganic, molecule/bulk interface that are commonly encountered in molecular electronics, photovoltaics, and photoelectrochemistry. The processes studied include the relaxation of the injected electron inside the TiO_2 conduction band (CB), the back electron transfer (ET) from TiO_2 to alizarin, the ET from the surface to the electrolyte, and the regeneration of the neutral chromophore by ET from the electrolyte to alizarin. Developing a theoretical understanding of these processes is crucial for improving solar cell design and optimizing photovoltaic current and voltage. The simulations carried out for the entire system that contains many electronic states reproduce the experimental time scales and provide detailed insights into the ET dynamics. In particular, they demonstrate the differences between the optimized geometric and electronic structure of the system at 0 K and the experimentally relevant structure at ambient temperature. The relaxation of the injected electron inside the TiO_2 CB, which affects the solar cell voltage, is shown to occur on a 100 fs time scale and occurs simultaneously with the electron delocalization into the semiconductor bulk. The transfer of the electron trapped at the surface to the ground state of alizarin proceeds on a 1 ps time scale and is facilitated by vibrational modes localized on alizarin. If the electrolyte mediator is capable of approaching the semiconductor surface, it can form a stable complex and short-circuit the cell by accepting the photoexcited electron on a subpicosecond time scale. The ET from TiO_2 to both alizarin and the electrolyte diminishes the solar cell current. Finally, the simulations show that the electrolyte can efficiently regenerate the neutral chromophore. This is true even though the two species do not form a chemical bond and, therefore, the electronic coupling between them is weaker than in the TiO_2−chromophore and TiO_2−electrolyte donor−acceptor pairs. The chromophore−electrolyte coupling can occur both directly through space and indirectly through bonding to the semiconductor surface. The ET events involving the electrolyte are promoted primarily by the electrolyte vibrational modes.

1. Introduction

For many years scientists have conducted a variety of experiments and developed a number of theoretical models to study the movement of charge in molecules and solid-state structures. Electron transfer (ET) across molecular/bulk interfaces, however, is still poorly understood, a deficit that is due to the fact that the two components of the interface are not only starkly different in themselves but also typically investigated by different disciplines: molecules which show finite sets of discrete, localized orbitals are typically studied by chemists; inorganic bulk materials which are characterized by continuous bands of delocalized quantum states are studied by physicists. The intrinsic differences between the electronic and vibrational states of the two systems, as well as the often disparate sets of theories and experimental tools used by chemists and physicists, create challenges for the study of the organic−inorganic interface. In responding to these challenges, many researchers have focused on molecular/bulk interfacial ET because of the central role it plays in several developing fields: charge transfer across the contacts remains the most important area of study in the burgeoning area of molecular electronics;[1−4] photoinduced ET at organic/inorganic interfaces constitutes a major focus of research in the chemistry of photoelectrolysis,[5,6] photocatalysis,[7,8] and color photography;[9] and interfacial ET is the primary step in many solar energy conversion devices, since it creates free charge carriers upon the absorption of a photon. The development of solar cells is a particularly lively area of research

(1) Nitzan, A.; Ratner, M. A. *Science* **2003**, *300*, 1384.
(2) Fan, F. F.; Yao, Y.; Cai, L.; Cheng, L.; Tour, J. M.; Bard, A. J. *J. Am. Chem. Soc.* **2004**, *126*, 4035.
(3) Zhirnov, V. V; Cavin, R. K. *Nat. Mater.* **2006**, *5*, 11.
(4) Li, B.; Zhao, J.; Onda, K.; Jordan, K. D.; Yang, J. L.; Petek, H. *Science* **2006**, *311*, 1436.
(5) Lewis, N. S. *J. Electroanal. Chem.* **2001**, *508*, 1.
(6) Memming, R. *Semiconductor Electrochemistry*; Wiley-VCH: Weinheim, 2001.
(7) Zhao, W.; Ma, W. H.; Chen, C. C.; Zhao, J. C.; Shuai, Z. G. *J. Am. Chem. Soc.* **2004**, *126*, 4782.
(8) Hirakawa, T.; Whitesell, J. K.; Fox, M. A. *J. Phys. Chem. B* **2004**, *108*, 10213.
(9) Liu, D.; Hug, G. L.; Kamat, P. V. *J. Phys. Chem.* **1995**, *99*, 16768.

10.1021/ja0707198 CCC: $37.00

in which a wide variety of new designs are being investigated, including dye-sensitized semiconductor solar cells,[10−16] assemblies of inorganic semiconductors with conjugated polymers,[17−20] as well as devices employing quantum dots,[21−23] fullerenes,[24,25] carbon nanotubes,[26,25,27] and other recently discovered materials.

Dye-sensitized semiconductor solar cells, or Grätzel cells, are particularly valuable systems to study. They form one of the most promising alternatives to the more costly traditional solar cells, and the chromophore−semiconductor interface that is their key component provides an excellent general case for investigating the organic/inorganic interfacial ET. The extensive experimental efforts devoted to characterizing the chemical structure, electronic properties, and electron-vibrational dynamics of dye−semiconductor systems[10−16,28−56] create a basis for the theoretical analysis of the general properties of the interface[34,35,57−61] and for detailed computer simulations of specific systems, which typically include a TiO_2 semiconductor surface and a chromophore.[62−72] The latter is either a relatively large organic molecule or a complex of a transition metal with smaller organic ligands.

The conversion of the solar energy into an electric current in the Grätzel cell starts with the photoexcitation of the chromophore from its ground state, which is located energetically in the semiconductor band gap, to an excited state that is resonant with the TiO_2 conduction band (CB) (Figure 1). After the excitation, an electron is injected from the chromophore to the semiconductor surface, typically on an ultrafast time scale, τ_i. The injection competes with intramolecular relaxation to lower energy excited states, such as the triplet states of the transition metal chromophores,[42,48] or back to the ground state. Following the transfer, the electron diffuses into the bulk, τ_d, simultaneously relaxing to the bottom of the CB and losing its energy to vibrations, τ_v in Figure 1. In order to complete the cell circuit it must then move to the electrode that is attached to the semiconductor, carry an electric load, reach the second electrode, and transfer to the cell mediator which carries it back to the chromophore ground state. Occasionally, the electron remains trapped at the surface. The trapping of the electron immediately after the injection becomes a factor if the relaxation inside the CB occurs faster than the delocalization into the bulk, and if the surface contains many defects or unsaturated bonds that support surface states. But surface trapping can be important even if the electron is able to diffuse into the bulk. In order to optimize light harvesting and maximize charge separation, the semiconductor is designed to have a high surface area with multiple chromophore adsorption sites. For instance, the semiconductor may be prepared as a collection of TiO_2 nanoparticles that have been sintered together. In that case, the injected electron is never far from the surface and can easily return to it before it reaches the electrode. The position of the electron relative to the surface determines whether it will reach the

(10) Oregan, B.; Grätzel, M. *Nature* **1991**, *353*, 737.
(11) Huang, S. Y.; Schlichthorl, G.; Nozik, A. J.; Gratzel, M.; Frank, A. J. *J. Phys. Chem. B* **1997**, *101*, 2576.
(12) McConnell, R. D. *Renew. Sustain. Energy Rev.* **2002**, *6*, 273.
(13) Tributsch, H. *Coord. Chem. Rev.* **2004**, *248*, 1511−30.
(14) Biju, V.; Micic, M.; Hu, D. H.; Lu, H. P. *J. Am. Chem. Soc.* **2004**, *126*, 9374.
(15) Anderson N. A.; Lian, T. Q. *Ann. Rev. Phys. Chem.* **2005**, 56, 491.
(16) Watson, D. F.; Meyer, G. J. *Ann. Rev. Phys. Chem.* **2005**, 56, 119−56.
(17) Anderson, N. A.; Hao, E. C.; Ai, X.; Hastings, G.; Lian, T. Q. *Chem. Phys. Lett.* **2001**, *347*, 304.
(18) Lonergan, M. *Ann. Rev. Phys. Chem.* **2004**, *55*, 257−98.
(19) Haque, S. A.; Palomares, E.; Cho, B. M.; Green, A. N. M.; Hirata, N.; Klug, D. R.; Durrant, J. R. *J. Am. Chem. Soc.* **2005**, *127*, 3456.
(20) Fourier S.; Colladet, K.; Cleij, T. J.; Lutsen, L.; Gelan, J.; Vanderzande, D.; Nguyen, L. H.; Neugebauer, H.; Sariciftci, S.; Aguirre, A.; Janssen, G.; Goovaerts, E. *Macromolecules* **2007**, *40*, 65.
(21) Nozik, A. J. *Annu. Rev. Phys. Chem.* **2001**, *52*, 193.
(22) Schaller R. D.; Klimov, V. I. *Phys. Rev. Lett.* **2004**, *92*, 186601.
(23) Kamisaka, H.; Kilina, S. V.; Yamashita, K.; Prezhdo, O. V. *Nano Lett.* **2006**, *6*, 2295.
(24) Scharber, M. C.; Wuhlbacher, D.; Koppe, M.; Denk, P.; Waldauf, C.; Heeger, A. J.; Brabec, C. L. *Adv. Mater.* **2006**, *18*, 789.
(25) Segura, J. L.; Martin, N.; Guldi, D. M. *Chem. Soc. Rev.* **2005**, *56*, 31−47.
(26) Kymakis, E.; Amaratunga, G. A. J. *App. Phys. Lett.* **2002**, 80, 112−14.
(27) Habenicht, B. F.; Craig, C. F.; Prezhdo, O. V. *Phys. Rev. Lett.* **2006**, *96*, 187401.
(28) Tachibana, Y.; Moser, J. E.; Grätzel, M.; Klug, D. R.; Durrant, J. R. *J. Phys. Chem. B* **1996**, *100*, 20056−20062.
(29) Liu, Y.; Dadap, J. I.; Zimdars, D.; Eisenthal, K. B. *J. Phys. Chem. B* **1999**, *103*, 2480.
(30) Ramakrishna, G.; Ghosh, H. N.; Singh, A. K.; Palit, D. K.; Mittal, J. P. *J. Phys. Chem. B* **2001**, *105*, 12786.
(31) Piotrowiak, P.; Galoppini, E.; Wei, Q.; Meyer, G. J.; Wiewior, R. *J. Am. Chem. Soc.* **2003**, *125*, 5278−79.
(32) Furube, A.; Katoh, R.; Hara, K.; Sato, T.; Murata, S.; Arakawa, H.; Tachiya, M. *J. Phys. Chem. B* **2005**, *109*, 16406−14.
(33) Hannappel, T.; Burfeindt, B.; Storck, W.; Willig, F. *J. Phys. Chem. B* **1997**, *101*, 6799.
(34) Ramakrishna, S.; Willig, F. *J. Phys. Chem. B* **2000**, *104*, 68.
(35) Ramakrishna, S.; Willig, F.; May, V.; Knorr, A. *J. Phys. Chem. B* **2003**, *107*, 607.
(36) Schwarzburg, K.; Ernstorfer, R.; Felber, S.; Willig, F. *Coord. Chem. Rev.* **2004**, *248*, 1259.
(37) Gundlach, L.; Felber, S.; Storck, W.; Galoppini E.; Wei, Q.; Willig, F. *Res. Chem. Interm.* **2005**, *31*, 39−46.
(38) Persson, P.; Lundqvist, M. J.; Ernstorfer, R.; Goddard, W. A.; Willig, F. *J. Chem. Theory Comput.* **2006**, *2*, 441−51.
(39) Ghosh, H. N.; Asbury, J. B.; Lian, T. Q. *J. Phys. Chem. B* **1998**, *102*, 6482−86.
(40) Asbury, J. B.; Ellingson, R. J.; Ghosh, H. N.; Nozik, A. J.; Ferrere, S.; Lian, T. *J. Phys. Chem. B* **1999**, *103*, 3110.
(41) Asbury, J. B.; Hao, E.; Wang, Y.; Lian, T. *J. Phys. Chem. B* **2000**, *104*, 11957−64.
(42) Asbury, J. B.; Hao, E. C.; Wang, Y. Q.; Ghosh, H. N.; Lian, T. Q. *J. Phys. Chem. B* **2001**, *105*, 4545.
(43) Anderson, N. A.; Hao, E.; Ai, X.; Hastings, G.; Lian, T. *Physica E* **2002**, *14*, 215.
(44) Asbury, J. B.; Anderson, N. A.; Hao, E.; Ai, X.; Lian, T. *J. Phys. Chem. B* **2003**, *107*, 7376.
(45) Wang, Y.; Hang, K.; Anderson, N. A.; Lian, T. *J. Phys. Chem. B* **2003**, *107*, 9434.
(46) Anderson N. A.; Lian, T. Q. *Coord. Chem. Rev.* **2004**, *248*, 1231.
(47) She, C. X.; Anderson, M. A.; Guo, J. C.; Liu, F.; Goh, W. H.; Chen, D. T.; Mohler, D. L.; Tian, Z. Q.; Hupp, J. T.; Lian, T. Q. *J. Phys. Chem. B* **2005**, *109*, 19345−55.
(48) Ai, A.; Anderson, N. A.; Guo, J. C.; Lian, T. Q. *J. Phys. Chem. B* **2005**, *109*, 7088.
(49) Trachibana, Y.; Haque, S. A.; Mercer, I. P.; Durrant, J. R.; Klug, D. R. *J. Phys. Chem. B* **2000**, *104*, 1198−1205.
(50) Ramakrishna, G.; Singh, A. K.; Palit, D. K.; Ghosh, H. N. *J. Phys. Chem. B* **2004**, *108*, 4775−47833.
(51) Ramakrishna, G.; Jose, D. A.; Kumar, D. K.; Das, A.; Palit, D. K.; Ghosh, H. N. *J. Phys. Chem. B* **2005**, *109*, 15445−15453.
(52) Huber, R.; Spoerlein, S.; Moser, J. E.; Grätzel, M.; Wachtveitl, J. *J. Phys. Chem. B* **2000**, *104*, 8995.
(53) Huber, R.; Moser, J. E.; Grätzel, M.; Wachtveitl, J. *J. Phys. Chem. B* **2002**, *106*, 6494.
(54) Matylitsky, V. V.; Lenz, M. O.; Wachtveitl, J. *J. Phys. Chem. B.* **2006**, *110*, 8372.
(55) Zhang, D. S.; Downing, J. A.; Knorr, F. J.; McHale, J. L. *J. Phys. Chem. B* **2006**, *110*, 21890.
(56) Pollard, J. A.; Zhang, D. S.; Downing, J. A.; Knorr, F. J.; McHale, J. L. *J. Phys. Chem. A* **2005**, *109*, 11443.
(57) Ramakrishna, S.; Willig, F.; May, V. *J. Chem. Phys.* **2001**, *115*, 2743−56.
(58) Wang, L. X; May, V. *J. Chem. Phys.* **2004**, *121*, 8039.
(59) Wang, L. X.; Willig, F.; May, V. *J. Chem. Phys.* **2006**, *124*, 014712.
(60) Thoss, M.; Kondov, I.; Wang, H. B. *Chem. Phys.* **2004**, *304*, 169.
(61) Kondov, I.; Thoss, M.; Wang, H. *J. Phys. Chem. A* **2006**, 110, 1364−74.
(62) Kondov, I.; Wang, H. B.; Thoss, M. *Int. J. Quant. Chem.* **2006**, *106*, 1291.
(63) Rego, L. G. C.; Batista, V. S. *J. Am. Chem. Soc.* **2003**, 125, 7989.
(64) Abuabara, S. G.; Rego, L. G. C; Batista, V. S. *J. Am. Chem. Soc.* **2005**, *127*, 18234.
(65) Stier, W.; Prezhdo, O. V. *J. Phys. Chem. B* **2002**, *106*, 8047.
(66) Stier, W.; Prezhdo, O. V. *Isr. J. Chem.* **2002**, *42*, 213.
(67) Stier, W.; Duncan, W. R.; Prezhdo, O. V. *Adv. Mater.* **2004**, 16, 240.
(68) Duncan, W. R.; Stier, W. M.; Prezhdo, O. V. *J. Am. Chem. Soc.* **2005**, *127*, 7941.
(69) Duncan W. R.; Prezhdo, O. V. *J. Phys. Chem. B* **2005**, *109*, 17998.
(70) Duncan W. R.; Prezhdo, O. V. *J. Phys. Chem. B* **2005**, *109*, 365.
(71) Craig, C. F.; Duncan, W. R.; Prezhdo, O. V. *Phys. Rev. Lett.* **2005**, *95*, 163001.
(72) Duncan, W. R.; Prezhdo, O. V. *Annu. Rev. Phys. Chem.* **2007**, *58*, 143.

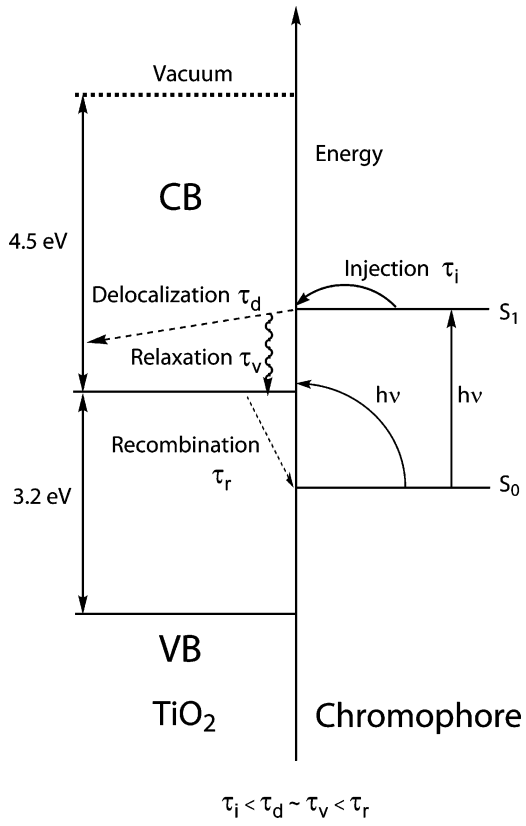

Figure 1. Energy diagram of the chromophore−TiO_2 interface. An absorbed photon promotes an electron from the ground state (S_0) of the dye, located in the semiconductor energy gap, into an excited state (S_1) that is in resonance with the CB. Typically, the dye excited state is well inside the CB. An additional direct photoexcitation from the dye ground state into a semiconductor state near the CB edge becomes possible with strong chromophore−semiconductor coupling. In some systems, such as alizarin-sensitized TiO_2, the dye excited state is located near the edge of the TiO_2 CB. Efficient electron injection into the edge of the CB avoids the energy and voltage loss by relaxation to the CB edge that is inevitable if injection occurs high in the CB. The injected electron delocalizes from the surface to the bulk, simultaneously relaxing to the bottom of the CB by coupling to vibrations. The electrons that return to or remain trapped at the surface recombine with the positive charges residing on the chromophore and with the electrolyte mediator.

electrode or whether it will short circuit the cell (τ_r) by recombining with the positive charge remaining on the chromophore after the injection or by transferring onto the electrolyte mediator. The mediator is located near the surface, since it brings electrons from the counter electrode in order to regenerate the neutral chromophore.

Clearly, the relative yields and rates of these processes influence the efficiency of the cell.[11−13] If the photoexcited electron decays to a low-energy chromophore state on a faster time scale than does the injection, or if the recombination at the surface is faster than the delocalization into the bulk, there will be very little current. Similarly, if an electron that has already reached the bulk returns to the surface and recombines with the chromophore or electrolyte, the current will be reduced. It is also a concern that electron relaxation to the band edge can decrease cell voltage. Developing a theoretical understanding of each of these processes is vital to the efficient improvement of solar devices. The electron injection is typically faster than the intramolecular relaxation to the ground electronic state; the latter rarely affects the cell performance. The role of the electron back transfer (back-ET), however, is particularly important. The relaxation and delocalization of the electron within the TiO_2 CB influence the back-ET rate and are also critical processes to understand.

Many experimentalists have investigated these issues in dye−TiO_2 systems by using time-resolved laser spectroscopies to monitor the electron evolution in real time. A particularly large body of work is devoted to the injection process.[15,28−48,52,53] The back-ET in these systems has been studied to a lesser extent, with the observed time scales ranging from subpicoseconds to milliseconds.[30,33,43,45,50−55] The faster rates occur when the diffusion into the bulk is limited, or when the electron is trapped at the surface. In comparing the charge-transfer dynamics in a catechol−TiO_2 nanoparticle system with those in the $Ti(catechol)_3^{2-}$ complex in solution, Lian and co-workers[45] observed a 200 fs back-ET process in the latter and a multicomponent back-ET process in the former. They attributed the fast 400 fs component that they observed with the nanoparticle system to electrons trapped at or near the initial Ti centers and the slow components to trapped states farther away. The time-resolved experiments of Ramakrishna et al., performed with the ruthenium−polypyridyl complexes strongly coupled to TiO_2 nanoparticles,[51] indicated that 30% of the injected electrons recombined with a time constant of less than 2 ps. The fastest back-ET component observed by the same group with quinizarin-sensitized TiO_2 was 600 fs, indicating that the charge separation lasts longer in the ruthenium-based systems than in organic dye-sensitized TiO_2 nanoparticles with similar dye−semiconductor interactions.[30,50] By comparing the back-ET dynamics involving ruthenium bipyridyl and porphyrin sensitizer dyes, Trachibana et al. concluded that the multiexponential nature of the recombination kinetics is not associated with properties of the sensitizer dye, but rather with heterogeneities and trap states in the TiO_2 film.[49]

Wachtveitl and co-workers[52−54] studied the back-ET in the alizarin/TiO_2 system, as well as alizarin/ZrO_2. In the TiO_2 system, which is the subject of our current work, they found multiphasic recombination dynamics within a wide range of time scales from 400 fs to nanoseconds. They tested the role of surface trap states by analyzing the dynamics in alizarin/ZrO_2. The bottom of the ZrO_2 CB is about 1.3 eV higher than the CB in TiO_2, and the excited state of the alizarin molecule is significantly below the ZrO_2 band edge. Following an ultrafast transfer from the chromophore to the surface trap states that occurred within less than 100 fs, the electron was unable to delocalize into the bulk, and it transferred back onto the dye, drastically enhancing the dye fluorescence.[52] The repopulation of the dye excited state took place within 450 fs; the subsequent relaxation to the ground state took 160 ps. Recently,[54] the Wachtveitl group studied injection and back-ET in the alizarin/TiO_2 system at a range of pH values. The pH change was enough to move the CB edge by 0.42 eV, and at higher pH the excited electrons were forced to inject into surface trap states; the injection was ultrafast across the entire pH range; and the back-ET showed multiphasic kinetics that depended on the acidity of the solution. In all pH values ranging from 2 to 9, the authors observed a picosecond back-ET component.

Electron back-transfer can also involve the cell electrolyte mediator. In general, the role of the redox mediator in the Grätzel cell is well-understood.[36,73] It takes an electron from the counter

(73) Kelly, C. A; Meyer, G. J. *Coord. Chem. Rev.* **2001**, *211*, 295.

electrode and brings it to the chromophore, reducing it and making it ready for the next photoexcitation/injection cycle. But the mediator can also affect the cell performance negatively by removing the photoexcited electron from the TiO_2 CB, causing a short circuit. The dynamics of the ET from the mediator to the chromophore and from TiO_2 to the mediator are harder to study by laser techniques than is the chromophore−TiO_2 ET, since the mediator is not chemically attached to its ET partners and it diffuses in and out of the reaction region. The ET rates involving the mediator should be very sensitive to the details of the diffusion process, such as the fluctuation of the distance to the chromophore or the semiconductor and the time spent in their vicinity. The structure of the solvent surrounding the ET reaction pair can play a critical role. Further complications may arise because the mediator that has approached the chromophore also lies in close proximity to the semiconductor.

The standard Grätzel cell uses the I^-/I_3^- redox pair electrolyte. Wijayantha and co-workers have argued that the dye-regeneration reaction involves $I_2^{\bullet -}$.[74] The intensity dependence of the electron lifetime that these authors observed was consistent with a second-order ET mechanism, leading to the following chemical scheme:

$$I_3^- \rightleftharpoons I_2 + I^-,\ K_1 \approx 10^{-7}\ \text{mol}\cdot\text{dm}^{-3}\ \text{in acetonitrile} \quad (1)$$

$$I_2 + e \rightleftharpoons I_2^{\bullet -},\ K_2$$

$$2I_2^{\bullet -} \xrightarrow{k_{disp}} I_3^- + I^-$$

$$I_2^{\bullet -} + e \xrightarrow{k_{ET}} 2I^-$$

The disproportionation reaction competes with the direct ET. The kinetics of both ET reactions involving I_2 neutral and $I_2^{\bullet -}$ anion match the experimental results.

A deep understanding of the various processes involved in interfacial charge transfer cannot be achieved without theoretical modeling that helps to clarify the underlying mechanisms and to interpret the experimental data. There are two different strategies for modeling the interfacial ET in real time: in one, fully quantum-mechanical electronic and vibrational dynamics are investigated using a simplified model of the interface,[34,35,57−61] and in the other, an explicit atomistic representation of the interface is combined with quantum-classical or semiclassical electron-vibrational dynamics.[63−72] Both strategies have their advantages: simplified models allow the authors to systematically vary the model parameters and to study the influence of various interface properties on the electron dynamics. Atomistic simulations, on the other hand, can treat a much more realistic interface, including the time-dependent geometric and electronic structure of the chromophore, the surface, and the chromophore surface binding.

In our previous work we performed *ab initio* time-domain atomistic simulations and investigated the rates and mechanisms of the electron injection.[65−72] We found that there was a competition between nonadiabatic (NA) and adiabatic types of ultrafast transfer. Adiabatic ET is mediated by a strong coupling between the chromophore and the semiconductor. During the transfer, the electron remains in the same adiabatic (Born−Oppenheimer) state that changes its localization from the dye to the semiconductor. In NA ET the electron quantum-mechanically hops (tunnels) between adiabatic states. The NA movement of charge from the dye to the semiconductor can occur at any nuclear configuration and is particularly important when the dye−semiconductor coupling is weak. The mechanism responsible for ET is relevant because the optimal conditions are in each case substantially different. NA transfer does not require a strong donor−acceptor interaction but relies rather on a high density of states (DOS) in the CB. Since a DOS grows with energy,[75] an increase of the chromophore excited-state energy relative to the CB edge will accelerate the NA transfer. At the same time, the photoexcitation energy and solar cell voltage will be lost due to the relaxation of the injected electron to the bottom of the CB. In the event of NA ET it is also important to minimize chromophore intramolecular vibrational relaxation, which lowers the chromophore energy and thereby the accessible DOS. The rate of NA ET will decrease exponentially with the increasing distance between the donor and acceptor species. Conversely, the adiabatic ET requires strong donor−acceptor coupling but depends much less on the density of acceptor states. Since adiabatic transfer requires an energy fluctuation that can bring the system to the transition state, a fast exchange of energy between vibrational modes of the chromophore will increase the likelihood of adiabatic ET. We found that in low-temperature simulations in which the photoexcited state was well within the CB and the chromophore was attached to the semiconductor via a carboxylic acid bridge, the NA mechanism dominated.[65] At room temperature,[66−71] the adiabatic mechanism accounted for the majority of ET, both for injection deep within the band occurring through the carboxylic acid bridge and for injection at the band edge occurring through a hydroxyl bridge. Unlike NA ET, which requires a large DOS, adiabatic ET can occur on an ultrafast time scale even at the band edge, where the DOS is much smaller. This discovery has the potential to help in the design of cells with higher voltages, since the voltage lost by the electron relaxation in the CB will be much smaller.[67] Our earlier results also indicate that the delocalization of the electron from the surface into the bulk takes on the order of 100 fs.[68]

In this paper we expand on our earlier work[65−72] and investigate the relaxation of the injected electron inside the TiO_2 CB, the back-ET from TiO_2 to alizarin, the transfer of the electron from the surface to the electrolyte, and the regeneration of the neutral chromophore. Following a description of our theoretical approach,[71] we consider the geometric and electronic structure of the interface optimized at zero Kelvin, study thermal fluctuations that substantially affect the interface electronic structure and activate atomic vibrations, and then focus on each relaxation process individually and as they occur in parallel.

2. Theory

This paper describes our real-time, fully atomistic simulations using the mixed quantum-classical approach[71] that combines time-dependent (TD) density functional theory (DFT)[76−79] with surface hopping

(74) Fisher, A. C.; Peter, L. M.; Ponomarev, E. A.; Walter, A. B; Wijayantha, K. G. U. *J. Phys. Chem. B* **2000**, *104*, 949.
(75) Kittel, C. *Introduction to solid state physics*; Wiley: New York, 1996.
(76) Marques, M. A. L.; Gross, E. K. U. *Annu. Rev. Phys. Chem.* **2004**, *55*, 427.
(77) Baer, R.; Neuhauser, D. *J. Chem. Phys.* **2004**, *121*, 9803.
(78) Tretiak, S.; Igumenshchev, K.; Chernyak, V. *Phys. Rev. B* **2005**, *71*, 033201.
(79) Li, X. S.; Frisch, M. J.; Tully, J. C.; Schlegel, H. B. *J. Chem. Phys.* **2005**, *123*, 084106.

(SH)[80−82] in the Kohn−Sham (KS) representation. The electrons are treated quantum mechanically by many-body DFT, and the nuclei, which are much heavier and slower, are treated classically. The following three subsections describe the TDDFT and SH components of the approach and provide simulation details.

2.1. Time-Dependent Kohn−Sham Theory for Electron−Nuclear Dynamics. The electron density is the central quantity in DFT.[76] It is represented within the Kohn−Sham (KS) approach[83] by the sum of the densities of the KS orbitals $\varphi_n(x,t)$ that are occupied by N_e electrons:

$$\rho(\mathbf{r},t) = \sum_{n=1}^{N_e} |\varphi_p(\mathbf{r},t)|^2 \tag{2}$$

The evolution of the electron density is derived by applying the TD variational principle to the KS energy,

$$E\{\varphi_p\} = \sum_{p=1}^{N_e} \langle\varphi_p|K|\varphi_p\rangle + \sum_{p=1}^{N_e} \langle\varphi_p|V|\varphi_p\rangle + \frac{e^2}{2}\int\int \frac{\rho(\mathbf{r}',t)\,\rho(\mathbf{r},t)}{|\mathbf{r}-\mathbf{r}'|}\,d^3\mathbf{r}d^3\mathbf{r}' + E_{xc}\{\rho\} \tag{3}$$

where the right-hand side consists of the kinetic energy, the electron−nuclear attraction, the electron−electron Coulomb repulsion, and the exchange-correlation energy functional. The TD variational principle gives a set of single particle equations for the evolution of the KS orbitals[76−79]

$$i\hbar\frac{\partial\varphi_p(\mathbf{r},t)}{\partial t} = H(\mathbf{r},\mathbf{R},t)\,\varphi_p(\mathbf{r},t), \qquad p = 1, 2, ..., N_e \tag{4}$$

in which the Hamiltonian depends on time through the external potential created by the vibrational motion of the nuclei. These equations are coupled, since the DFT functional, H, is dependent on the total electron density $\rho(\mathbf{r},t)$, eq 2.

The TD one-electron wavefunctions $\varphi_p(\mathbf{r},t)$ are expanded on the basis of adiabatic KS orbitals $\tilde{\varphi}_k(\mathbf{r};\mathbf{R}(t))$ that we obtain by a time-independent DFT calculation for the current atomic positions; this process will be detailed below. In particular, the KS orbital that corresponds to the photoexcited (PE) state is expanded as

$$\varphi_{PE}(\mathbf{r},t) = \sum_k c_{nk}(t)\,\tilde{\varphi}_k(\mathbf{r};\,\mathbf{R}(t)) \tag{5}$$

Inserting this equation into the TD KS eq 4 gives the evolution of the expansion coefficients

$$i\hbar\frac{\partial}{\partial t}c_j(t) = \sum_k c_k(t)\,(\epsilon_k\delta_{jk} + d_{jk}) \tag{6}$$

where ϵ_k is the energy of the adiabatic KS orbital k, and d_{jk} is the NA coupling between orbitals j and k. Atomic motions produce the parametric dependence of the adiabatic KS orbitals on time and determine the NA coupling. We calculate d_{jk} numerically as the overlap of orbitals j and k at sequential time steps[81]

$$d_{jk} = -i\hbar\langle\,\tilde{\varphi}_j\,|\nabla_{\mathbf{R}}|\,\tilde{\varphi}_k\rangle\cdot\frac{d\mathbf{R}}{dt} = -\hbar\left\langle\,\tilde{\varphi}_j\left|\frac{\partial}{\partial t}\right|\tilde{\varphi}_k\right\rangle \approx -\frac{i\hbar}{2\Delta t}(\langle\,\tilde{\varphi}_j(t)|\,\tilde{\varphi}_k(t+\Delta t))\rangle - \langle\,\tilde{\varphi}_j(t+\Delta t)|\,\tilde{\varphi}_k(t))\rangle) \tag{7}$$

Using these values for the NA coupling, we propagate eq 4 with the second-order differencing scheme[84] using a 10^{-3} fs time step.

In order to use these equations to monitor the alizarin/TiO_2 system, we make the following assumptions: First, in our TDDFT calculations we apply the PW91 exchange-correlation functional,[85] whose kernel is independent of the frequency of the TD external potential. Frequency dependent DFT kernels[86] are important for describing relatively large density changes that result from electronic excitations. But since our system is large, the excitation of a single electron has a relatively small effect on the total electron density. This allows us to neglect the frequency effects and assume that the time dependence of the kernel arises solely as a result of the time dependence of the electron density, which is smooth and driven by the external potential of the nuclei. Second, we assume that the ET dynamics are well represented in the single-electron orbital picture. This assumption is based on the following facts: Both the linear-response TDDFT calculations and the configuration interaction singles[70] calculations indicate that the lowest energy state in the alizarin−TiO_2 system is dominated by an electronic transition from the highest occupied molecular orbital (HOMO) to a virtual orbital that best matches the lowest unoccupied molecular orbital (LUMO) of free alizarin. Therefore, we model the photoexcitation by promoting an electron from the HOMO to this virtual orbital. Further, we focus on the evolution of the single electron that is promoted by the photoexcitation. It is this PE electron that determines the changes in the total electron density that are reflected in the electron injection, relaxation, and back-transfer. The other electrons, which are all in states below the CB, can be ignored; with the exception of the electron in the I_2^- state, they have no empty states below them to transfer to, and the empty states above them are too energetically distant. In particular (see Figure 1) the valence band (VB) of TiO_2 is well below the HOMO and virtual orbitals that represent the ground and excited states of alizarin, and the second electron that remains in the HOMO can neither relax down to the VB, which contains no empty orbitals, nor be excited to the CB, since such excitation requires far more energy than is available at room temperature. Analogous arguments apply to the states of the redox mediator, which are sufficiently below the CB to make upward transitions unlikely. In cases involving I_2^-, we treat the transfer of the electron from the mediator to the chromophore HOMO separately from the relaxation of the PE electron; the justification for this separation is detailed in the results section.

2.2. Fewest Switching Surface Hopping. Fewest switches surface hopping (FSSH) is a popular and well-tested approach to NA molecular dynamics (MD). Designed[80] to account for chemical reaction branching in condensed phase systems, FSSH satisfies detailed balance,[82] which ensures that the rates of the quantum transitions upward and downward in energy are related through the Boltzmann factor. The detailed balance condition leads to thermodynamics equilibrium and is essential for studies of relaxation processes. FSSH can be viewed as a quantum master equation where the electronic transition rates are dependent on time and atomic coordinates. The explicit time dependence of the FSSH transition probabilities properly accounts for the short-time behavior of the electronic transition processes, which can lead to the quantum Zeno and anti-Zeno effects.[87−89] The dependence of the transition probabilities on the atomic coordinates creates a correlation between the nuclear and electronic dynamics. In comparison to FSSH, the Ehrenfest approach,[79] which is one of the oldest and most straightforward NAMD methods, cannot be interpreted as a master equation. It presents a coherent electronic evolution that can produce neither detailed balance nor energy relaxation.[82,90,91]

(80) Tully, J. C. *J. Chem. Phys.* **1990**, *93*, 1061.
(81) Hammes-Schiffer, S.; Tully, J. C. *J. Chem. Phys.* **1994**, 101, 4657.
(82) Parandekar, P. V.; Tully, J. C. *J. Chem. Phys.* **2006**, *122*, 094102.
(83) Kohn, W.; Sham, L. J. *Phys. Rev.* **1965**, *140*, 1133.
(84) Leforestier, C.; Bisseling, R. H.; Cerjan, C.; Feit, M. D.; Friesner, R.; Guldberg, A.; Hammerich, A.; Jolicard, G.; Karrlein, W.; Meyer, H. D.; Lipkin, N.; Roncero, O; Kosloff, R. *J. Comput. Phys.* **1991**, *94*, 59.
(85) Perdew, J. P.; Burke, K.; Wang, Y. *Phys. Rev. B* **1996**, *54*, 16533.
(86) Onida, G.; Reining, L.; Rubio, A. *Rev. Mod. Phys.* **2002**, 74, 601.
(87) Prezhdo O. V.; Rossky, P. J. *Phys. Rev. Lett.* **1998**, *81*, 5294.
(88) Prezhdo, O. V. *J. Chem. Phys.* **1999**, *111*, 8366.
(89) Prezhdo, O. V. *Phys. Rev. Lett.* **2000**, *85*, 4413.

The probability of hopping from state j to state k during the time step δt is given in the FSSH by[80]

$$g_{jk}(t,\delta t) = \max\left(0, \frac{b_{kj}\delta t}{a_{jj}(t)}\right) \tag{8}$$

where

$$a_{kj}(t) = c_k(t)\, c_j(t) \text{ and}$$
$$b_{kj} = 2\hbar^{-1} Im(a_{kj} \langle \tilde{\varphi}_k | H | \tilde{\varphi}_j \rangle) - 2Re(a_{kj}\, \mathbf{d}_{kj}) \tag{9}$$

If the calculated g_{jk} is negative, the hopping probability is set to zero; a hop from state j to state k can occur only when the electronic occupation of state j decreases and the occupation of state k increases. Since we use an adiabatic KS representation, and the adiabatic KS orbitals are eigenfunctions of H, the imaginary term in eq 9 vanishes. In the standard formulation of FSSH, the nuclear velocities are rescaled after a hop to conserve the total energy of electrons and nuclei.[80,81] If the kinetic energy available to the nuclei along the direction of the NA coupling is insufficient to accommodate an increase in the electronic energy, the hop is rejected. The hop rejection is responsible for detailed balance between upward and downward transitions.[82]

The current, simplified implementation of FSSH makes the assumption that the energy exchanged between the electronic and vibrational degrees of freedom during the hop is rapidly redistributed among all vibrational modes. Under this assumption, the distribution of energy in the vibrational modes is Boltzmann at all times, and the velocity rescaling plus hop rejection can be replaced by multiplying the probability (8) for transitions upward in energy by the Boltzmann factor. This simplification significantly increases the computational efficiency of the method and allows us to use the ground state atomic trajectory in order to determine the TD potential that drives the electron dynamics, eq 6.

2.3. Simulation Details. In order to capture all of the important processes—the electron injection from the dye to the CB; the relaxation in the CB; the back-ET from the TiO_2 surface to the dye; and the ET involving the mediator—we functionalize the surface to produce four different systems: (a) alizarin/TiO_2; (b) I_2/TiO_2; (3) I_2^-/TiO_2; and (4) alizarin/I_2^-/TiO_2 (Figure 2). The simulation cells contain a slab of TiO_2 that is five layers thick, with the bottom two layers frozen in the bulk configuration. Both surfaces are terminated by hydroxyl groups, which are attached to the titaniums, and by hydrogens, which are attached to the bridging oxygens.[92] Periodic boundary conditions create an array of slabs, but a vacuum above each surface keeps the slabs from interacting with each other. This structure results in a cell with the dimensions $9.3 \times 9.3 \times 30$ Å^3. The electronic properties of the systems are calculated by DFT with the VASP code.[93,94] The periodic boundary conditions and plane wave basis sets that are used in the code are especially effective for semiconductors and other extended periodic systems. The core electrons are simulated using the Vanderbilt pseudopotentials,[95] and only the valence electrons are treated explicitly.

The assembled structures of the chromophore and redox mediator on the TiO_2 surface are optimized at zero Kelvin first, and then are brought to equilibrium at ambient temperature by repeated velocity rescaling. A 1 fs MD time step is used for both equilibration and the subsequent production runs. Upon equilibration, an adiabatic ground state trajectory is generated in the microcanonical ensemble. The adiabatic state energies and NA couplings are computed for each of the steps of the production run. Multiple configurations are harvested from the production run and are used as initial configurations of the system at the time of the photoexcitation. For each configuration in systems with alizarin the KS orbital corresponding to the photoexcited state is chosen by selecting the adiabatic state with the largest localization in the portion of the simulation cell that is occupied by the dye. The selection of the initial state in the I_2^-/TiO_2 system without the chromophore (Figure 2c) is detailed in the results section. An electron is promoted from an occupied orbital to the PE state orbital, and an NAMD run is initiated.

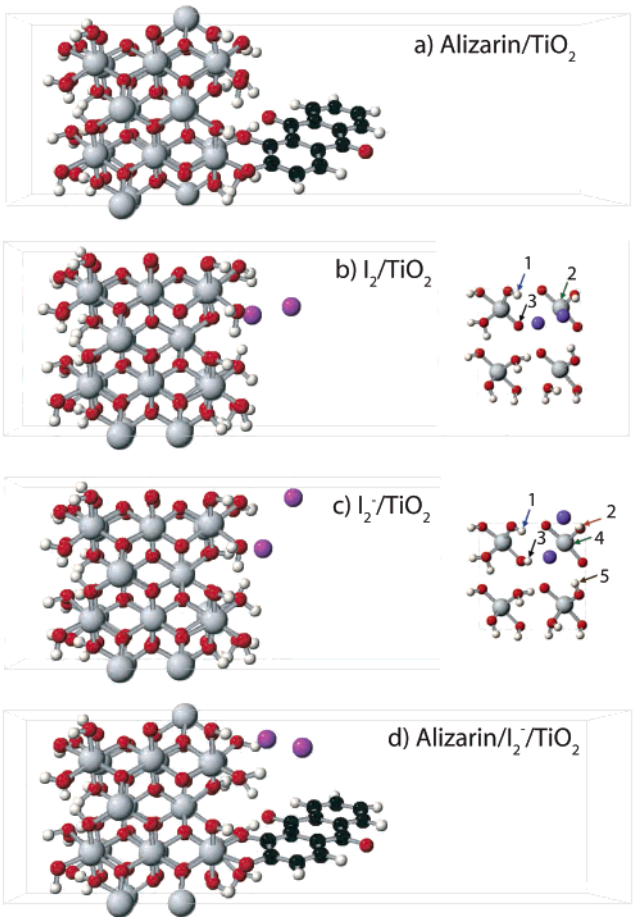

Figure 2. Simulations cells showing the optimized geometries of the alizarin/TiO_2, I_2 /TiO_2, I_2^-/TiO_2, and alizarin/I_2^-/TiO_2 systems. The atoms are denoted as follows: Ti, large gray; O, red; C, black; H, white; I, larger purple. The dangling bonds of the TiO_2 surface are saturated by H^+ and OH^- groups, as expected in solution or ambient humidity. Alizarin attaches to the semiconductor through Ti−O chemical bonds created between the surface and the chromophore by loss of a water molecule. Neutral I_2 also replaces a surface water molecule. I_2 is weakly bound and dissociates off the surface upon heating to room temperature. The I_2^- anion replaces OH^- but is too big to fit within the space vacated by the hydroxyl group. I_2^- stays bound to the positively charged surface hydrogens and leans toward the surface in order to maximize the electrostatic interaction of the surface with both iodine atoms. The arrows in the inserts in parts (b) and (c) indicate the surface atoms that are most strongly interacting with the iodines. The I_2^- anion is placed close to the alizarin molecule in the combined alizarin/I_2^- system, as expected when the electron injection creates positively charged alizarin.

3. Results and Discussion

The *ab initio* time-domain simulations of the photoinduced electron dynamics at the chromophore−semiconductor interface, both with and without the redox mediator, create a detailed real-time atomistic picture of the charge transfer and relaxation processes. The following discussion emphasizes several issues that are related to the electron dynamics: the geometric structure

(90) Horsfield, A. P.; Bowler, D. R.; Fisher, A. J.; Todorov, T. N.; Sanchez, C. G. *J. Phys.: Condens. Matter* **2004**, *16*, 8251.
(91) Prezhdo, O. V. *Theor. Chem. Acc.* **2006**, *116*, 206.
(92) Zhang, Z., et al. *Langmuir* **2004**, *20*, 4954.
(93) Kresse, G.; Furthmüller, J. *Comput. Mater. Sci.* **1996**, *6*, 15.
(94) Kresse, G.; Furthmüller, J. *Phys. Rev. B* **1996**, *54*, 11169.
(95) Vanderbilt, D. *Phys. Rev. B* **1990**, *41*, 7892.

Scheme 1

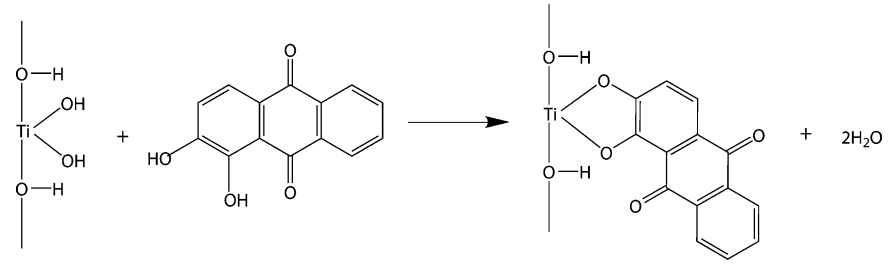

Scheme 2

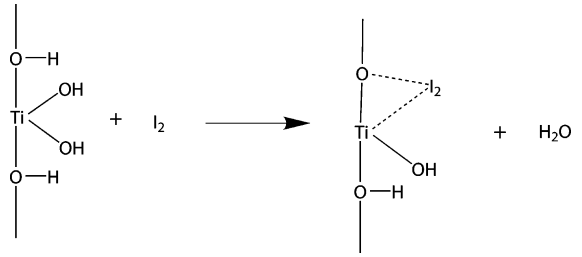

Scheme 3

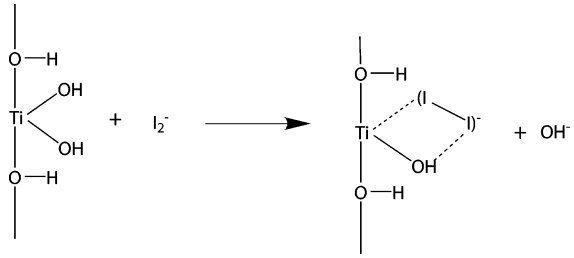

of the interface; the differences in the interface electronic structure at 0 K and at room temperature; the relaxation of the electron inside the TiO_2 CB; the back-ET onto the dye and the redox mediator in systems with only the dye, in systems with only the mediator, and in systems with both species; and the ET from the mediator to the dye.

3.1. Geometric Structure of the Chromophore−Semiconductor Interface in the Presence of the Redox Mediator. The position and orientation of the chromophore and redox mediator relative to the TiO_2 surface determine the strength of the interfacial interactions and, therefore, the rates and yields of the ET processes. Alizarin molecules bind to TiO_2 through the interaction of electron pairs on the hydroxyl oxygens in alizarin with the d-orbitals of Ti atoms (Figure 2a). The feasible binding motifs include molecular adsorption and chemical binding through one Ti−O bond, through two Ti−O bonds directed at a single Ti atom or two separate ones, as well as a number of possibilities involving tautomerism and hydrogen migration in alizarin. Among these motifs, the most stable geometry corresponds to the bidentate structure that has two chemical bonds directed to the same surface titanium. This conclusion follows from the *ab initio* molecular orbital and DFT studies by Thurnauer's group[96] on the related catechol molecule. The alizarin tautomeric structures associated with hydrogen migration between the hydroxyl and the carboxyl group are not possible with catechol; however, the tautomerism destabilizes the molecular π-system and requires additional energy. The present study uses bidentate binding (Figure 2). The bonds are formed by the loss of a water molecule from the saturated surface (Scheme 1). The redox mediator can accept the electron from the TiO_2 surface in both neutral I_2 and ionic I_2^- forms following the reaction shown in Scheme 1. In order to closely approach the surface, the I_2 molecule must displace a water molecule (Scheme 2), keeping the overall system neutral. Since the titanium atoms are more deeply buried below the surface than are the oxygen atoms, the I_2 molecule has a better chance of interacting with the oxygens (Figure 2b). Indeed, the iodine that is closest to the surface is located 2.50 Å from the bridging oxygen from which the hydrogen was removed to form the water molecule—black 3 arrow in Figure 2b insert—and 3.21 Å from the titanium that is missing the hydroxyl group—green 2 arrow. The I_2−surface interaction is further enhanced by a hydroxyl group hydrogen that is 2.53 Å from the iodine atom—blue 1 arrow. The I−I distance is 2.80 Å, and the bond axis is pointed toward the oxygen. The iodine atom that is farther from the surface is tilted in the direction of the titanium, making an angle of around 50° between the I−I bond and the surface.

The anionic form of the mediator I_2^- reaches the surface by replacing a hydroxyl group (Scheme 3). Here the I−I distance is 3.25 Å (Figure 2c), substantially longer than in neutral I_2. This increase is to be expected, since the extra electron occupies a π antibonding orbital. The distance to the closest titanium, the one with the missing hydroxyl group, is 3.36 Å—green 4 arrow in Figure 2c insert—which is larger than that for neutral I_2. The stronger interaction between I_2^- and the surface is facilitated by the surface hydrogens; the iodine atom closest to the surface simultaneously interacts with three separate hydrogens: the one connected to the bridging oxygen—2.43 Å, black 3 arrow—and two from surface bound hydroxyl groups—2.75 Å, brown 5 arrow and 2.88 Å, blue 1 arrow. The I−I bond is substantially tilted toward the surface, such that the iodine atom that is farther from the surface is close to two hydroxyl hydrogens—2.46 Å, orange 2 arrow—and 2.64 Å, not marked, since it is in the neighboring image of the simulation cell. The closer one is attached to the Ti with the missing hydroxyl group. The association of I_2^- with the hydrogens on the surface is to be expected, since the I_2^- molecule is too big to fit inside the space vacated by the hydroxyl group, and since the I_2^- negative charge interacts with the partial positive charges of the hydrogens.

In the combined system, I_2^- interacts with both the TiO_2 surface and alizarin (Figure 2d). The I−I bond is 3.23 Å, which is similar to the bond length in the I_2^- that is attached to the bare surface (Figure 2c). The distance between the iodine atom that is closest to the surface and the titanium atom that is missing the hydroxyl group is 3.28 Å. The closest hydrogen attached to a bridging oxygen is 3.46 Å away from I_2^-. Again, two hydroxyl hydrogens have close associations with the surface iodine, 2.44

(96) Redfern, P. C.; Zapol, P.; Curtiss, L. A.; Rajh, T; Thurnauer, M. C. *J. Phys. Chem. B* **2003**, *107*, 11419.

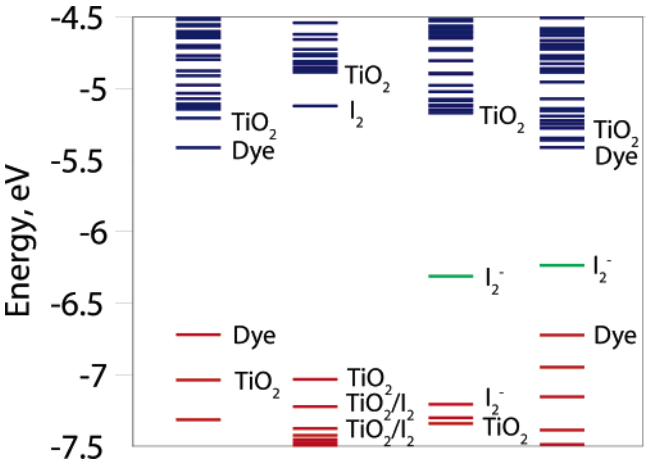

Figure 3. Energy diagrams involving the key states in the alizarin/TiO_2, I_2/TiO_2, I_2^-/TiO_2, and alizarin/I_2^-/TiO_2 systems with optimized geometries, Figure 2. The doubly and singly occupied and vacant states are denoted by red, green, and blue bars (gray, light gray, and black in black-and-white), respectively. The alizarin excited-state is located slightly below the TiO_2 CB, while the alizarin ground state is well inside the band gap and is closer to the TiO_2 VB. The lowest energy vacant state of I_2-neutral is also slightly below the TiO_2 CB edge, while the I_2 ground state is inside the VB. The I_2^- anion singly occupied state is in the middle of the TiO_2 band gap. The TiO_2 surface state energies are notably perturbed in the combined system, such that the CB edge moves down, closer to the alizarin excited state. Room-temperature fluctuations in the atomic coordinates have a significant effect on the state energies, as illustrated below in Figure 6.

Å and 2.98 Å. The iodine that is farther away is associated with hydrogens from surface hydroxyl groups; the distances are 2.39 Å and 2.67 Å. The interaction between I_2^- and alizarin occurs through the upper iodine atom, which is attracted by the positively charged chromophore hydrogens and approaches within 3.24 Å of them.

3.2. Electronic Structure of the Interface at 0 K. The electron injection, relaxation, and back-transfer dynamics depend on the energies of the electronic states and the coupling between the donor and acceptor levels. The strength of the coupling is directly reflected by the amount of mixing between the donor and acceptor orbitals. The energies of the electronic states for the four interfacial systems in their optimal geometric structures (Figure 2) are presented in Figure 3. Note that the TiO_2 CB edge is at slightly different positions in each system. While further calculations could determine the common zero point, we were interested only in the relative energies within each system, since the relative energies are what determine the electron dynamics. The calculated energy gaps are notably smaller than the experimental values; in the I_2^-/TiO_2 system the calculated TiO_2 band gap is 2.1 eV, and in the combined system the energy difference between the alizarin HOMO and LUMO is 1.31 eV, while the experimental values are 3.2 eV for bulk TiO_2 and 2.46 eV for the alizarin first excitation energy.[52] This is expected with Kohn−Sham energy gaps and DFT functionals that do not include exact exchange interaction. Since the evolution of the PE electron depends on the relative state energies, these errors could potentially give us overly fast transfer times. We address this issue by comparing the time scales of electron relaxation and back transfer in systems with these artificially small energy gaps, as well as in systems where the energy gaps have been changed to match the experimental values.

The excitation energies can be evaluated more rigorously when using the same set of KS orbitals by promoting an electron between the corresponding pair of orbitals, computing the total energy of the system with the promoted electron, and subtracting the total ground state energy. This procedure gives better agreement with experiment, in particular the calculated TiO_2 band gap, which in I_2^-/TiO_2 is 2.58 eV, while the alizarin first excitation energy in the combined system is 1.54 eV. Although the more rigorous approach improves the energies, it requires an additional calculation for each of the 40 excited states and is therefore not computationally feasible to perform over a several picosecond MD trajectory. The NA coupling between the many-electron states that produce the total energies are determined by the NA coupling between the corresponding pair of orbitals.[71] Therefore, the values of the coupling are computed at the same level of rigor as the total energies. Since the excessive computational cost make it impractical to obtain the total energy differences, we chose to scale the energy gaps based on the experimental data, as described below.

In comparing the electronic structure of the I_2 /TiO_2 and I_2^-/TiO_2 systems, we note that the singly occupied I_2^- orbital that accepts the PE electron from the semiconductor is lower in energy than the corresponding vacant orbital of neutral I_2. This is because the I_2^- orbital already contains an electron, which lowers its energy. Additional stabilization takes place by the interaction of I_2^- with a number of positively charged surface hydrogens. In the system with just alizarin, the alizarin excited state is located slightly below the TiO_2 CB, while the alizarin ground state is well inside the band gap and is closer to the TiO_2 VB. Whether or not the first excited state of alizarin is just below or just above the edge of the TiO_2 CB has not been determined unambiguously. Calculations using different DFT functionals produce a range of results,[62,70] while the experimental red shift[52] of the spectrum of surface-bound alizarin relative to free alizarin indicates only that there are significantly more TiO_2 states above than below the alizarin excited state. The experimentally observed[53] efficient electron injection from alizarin into TiO_2, together with the strong chromophore−semiconductor coupling and the predominantly adiabatic injection mechanism,[67,68] show that the alizarin excited state is within k_BT of the TiO_2 CB at room temperature.

Including both alizarin and I_2^- in the combined system affects the states for both surface-bound species; the I_2^- state moves closer to the CB, and while the alizarin HOMO−LUMO gap remains the same, both alizarin states are also pushed upward relative to the CB. By bringing the energies of the adsorbed species close to the CB, this cooperativity effect can be expected to speed up the electron injection from alizarin to TiO_2, the back-ET from TiO_2 to alizarin, and the ET from TiO_2 to the redox mediator. Since all of the systems have a net zero charge, the effect is real, rather than due to some spurious charge that is built up in the simulation cell.

As we have discussed in previous articles[67,68] the HOMO and LUMO orbitals of the alizarin/TiO_2 system in the optimized structure do not mix appreciably with the semiconductor states, because they are in the TiO_2 band gap (Figure 4). They are, therefore, very similar to the orbitals for free alizarin and lead to very similar optical excitation energies.[70] The HOMO and LUMO of alizarin as computed by DFT are also very similar to the corresponding Hartree−Fock orbitals,[70] which have a better defined physical interpretation and a more rigorous relationship to the optical excitation energies.[97] The HOMO is

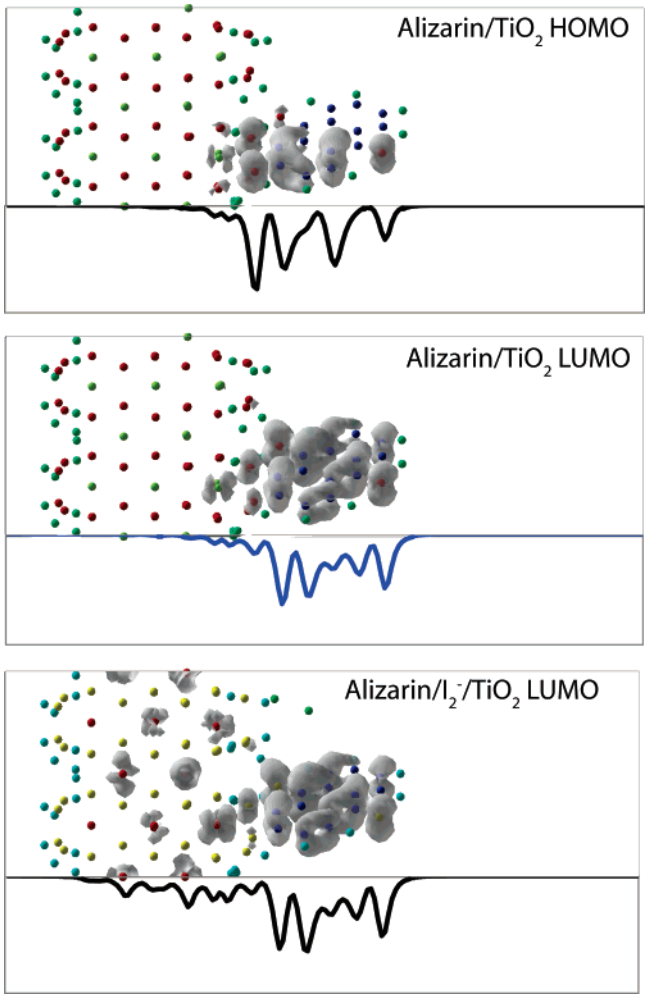

Figure 4. HOMO and LUMO of the alizarin/TiO_2 and LUMO of the combined alizarin/I_2^-/TiO_2 system. The top part of each panel shows the electron density, while the bottom part depicts the projection of the density onto the normal to the surface. The π-electron HOMO and π*-electron LUMO of bound alizarin are very similar to the free alizarin HOMO and LUMO because the dye states are in the semiconductor band gap, Figure 3, and do not mix appreciably with the TiO_2 states. The LUMO in the system that includes both alizarin and I_2^- is also similar to the free dye orbital. However, there is a significant amount of mixing with the TiO_2 CB states that are formed by Ti d-orbitals, as should be expected due to the energetic proximity of the alizarin excited state to the TiO_2 CB.

a π orbital localized toward the hydroxyl end of the molecule with a small amount of density on the surface titanium to which the dye is attached. The LUMO is evenly delocalized over the molecule, again with a very small amount on the semiconductor surface. Even though the orbitals obtained for the optimized geometry are well localized on the dye, the degree of delocalization onto the surface changes during the course of the dynamics simulations, since thermal fluctuations can move the orbital into the CB, where it spreads over a series of CB states. In the I_2^-/alizarin system, the alizarin LUMO state is already relatively delocalized into the TiO_2 slab, even in the geometry-optimized configuration, since the alizarin LUMO is pushed into the CB. The semiconductor states with which it mixes are made up of Ti d-orbitals. The integrated charge density that is shown below the orbital has two peaks for the second and fourth titanium layers because of the alternating orientation of the orbitals that maximizes their overlap.

The combined system also exhibits more interaction between the I_2^- state and the semiconductor than that in I_2^-/TiO_2 (Figure 5). This can be seen from the fact that there is more density on the surface near the I_2^- in the combined system. The integration of the charge density also shows a shift of density toward the surface along the I−I bond.

3.3. Electronic Structure of the Interface at Room Temperature. The thermal energy of vibrational motion has a dramatic effect on the electronic and even on the geometric structure of the interface at room temperature. First, the binding energy between neutral I_2 and the TiO_2 surface is smaller than k_BT, and as a result, the I_2 molecule dissociates from the surface. At the same time, the I_2 state energy, which is close to the CB when I_2 is attached to the surface, drifts downward, away from the CB edge. Second, thermal fluctuations in the atomic positions increase the energies of the alizarin excited state and of the I_2^- orbital that accepts the electron, relative to the CB edge; compare Figure 6 with Figure 3. The effect is surprising, since *a priori* one can expect fluctuations around the zero temperature values, and can be rationalized by considering the qualitative dependence of the electronic state energies on the atomic coordinates. The energies are at their lowest in the optimized geometry and tend to increase due to thermal distortions of the optimized geometry. Since the TiO_2 states are delocalized over many atoms, they are less sensitive to the displacement of the atoms than the I_2, I_2^-, and alizarin states, which are localized over a finite number of atoms. Therefore, thermal vibrational fluctuations do not appreciably affect the TiO_2 CB but do raise the energy of the molecular electronic states.

The increase of the alizarin and of the I_2^- state energies has important implications for the electron dynamics. The alizarin state is now inside the CB more often, and therefore, it has a chance to interact and mix with the TiO_2 states, increasing the degree of delocalization of the PE state onto the semiconductor. The thermal oscillations of the alizarin state energy move this state across the CB edge and dictate the injection dynamics.[66−68] The approach of the I_2^- state energy to the edge of the TiO_2 CB can be expected to facilitate ET onto the mediator. The state energy fluctuation of I_2^- is slower than that of alizarin, 400 fs vs 50 fs, and proceeds with a large amplitude, about 0.5 eV. In the combined system, instead of moving closer to the CB, the I_2^- state moves further away. In all cases, the thermal fluctuations have a much smaller effect on the TiO_2 states, as is expected for orbitals that are delocalized over a large volume.

3.4. Vibrational Motions Driving Electron Dynamics. The frequencies of the atomic vibrations that determine the oscillations of the electronic energies are detailed in Figure 7, which shows the spectral densities—the Fourier Transforms (FTs) of the autocorrelation functions—for the PE state−HOMO(alizarin) gap in alizarin/TiO_2, the CB edge−HOMO(alizarin) gap in alizarin/TiO_2, the CB edge−HOMO(I_2^-) gap in I_2^-/TiO_2, and the HOMO(I_2^-)−HOMO-1(alizarin) gap in alizarin/I_2^-/TiO_2. The alizarin PE state−HOMO gap fluctuations reflect the vibrations that participate in the intramolecular relaxation. They have a stronger dependence on the higher frequency C−C stretches and bends than do the fluctuations of the PE state energy alone, which influence the injection process.[68] The difference in energy between the two states has a stronger

(97) Szabo, A; Ostlund, N. S. *Modern Quantum Chemsitry*, 1st revised ed.; McGraw-Hill, Inc.: New York, 1989.

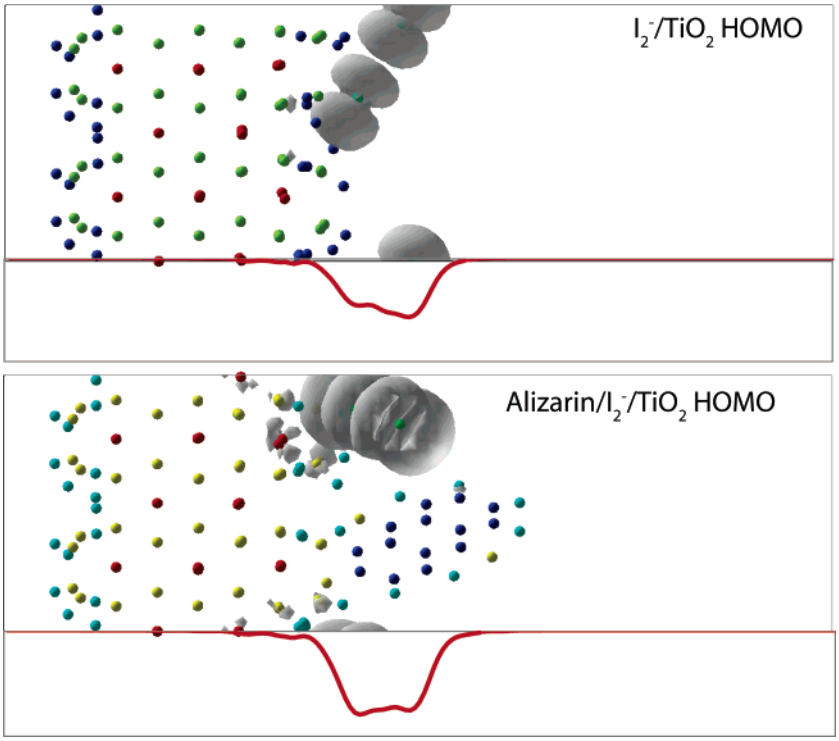

Figure 5. HOMO of the I_2^-/TiO_2 and alizarin/I_2^-/TiO_2 systems. The top part of each panel shows the electron density, while the bottom part depicts the projection of the density onto the normal to the surface. The HOMOs are formed by p-electrons of the iodine atoms. The density is higher on the outside iodine atom in the I_2^-/TiO_2 system and on the inside iodine atom in the combined system, as evidenced by the density projections. The I_2^- state of the combined system shows more mixing with the TiO_2 surface states.

oscillation at higher frequencies than does either state alone, and it has weaker oscillations at lower frequencies than the individual states because the energy fluctuations of the PE state and the HOMO are more out of phase for high-frequency motions than they are for low-frequency motions.

In general, the fluctuations of the CB edge−alizarin HOMO energy gap reflect the vibrations that participate in back-ET to the chromophore. Because the TiO_2 state energy oscillations are so small relative to alizarin's, the FT of the CB edge−alizarin HOMO energy gap essentially represents a single state energy fluctuation; it is very similar to the spectral density of the alizarin HOMO state, which is not shown in the figure. It is also much more similar to the PE state FT than it is to the alizarin PE state−HOMO gap FT; the dominant frequencies are at midrange energies with the largest peak corresponding to 690 cm^{-1}. These midrange frequencies dominate because the alizarin HOMO state is more delocalized across the dye than the PE state, which occupies only a third of the chromophore. In the alizarin system, the PE state is often below the CB edge, and therefore the fluctuations of the PE state−HOMO gap also play a role in the back-ET to the dye. There are fewer midrange frequencies present, but high-energy and low-energy oscillations have large amplitudes.

The spectral density of the CB edge−HOMO(I_2^-) gap in I_2^-/TiO_2, third panel in Figure 7, highlights the vibrations that play an active part in the ET from the semiconductor to the electrolyte. The only significant peaks are at frequencies below 100 cm^{-1} and are due to I_2^- bends relative to the surface and the I−I stretch.[98] The largest peak at 85 cm^{-1} corresponds to the 400 fs oscillation in the I_2^- energy, which is prominent in the trajectory shown in Figure 6b and is due to the I_2^- stretching mode. In comparing the back-ET from TiO_2 to the chromophore, the CB edge−alizarin HOMO gap FT, and the electrolyte to the chromophore, the CBedge−HOMO(I_2^-) gap FT, one observes that the back-ET to the electrolyte is promoted by much slower modes. Therefore, one may expect that the NA coupling between the TiO_2 and I_2^- states should be weaker than that between TiO_2 and alizarin. In either case, vibrations of the semiconductor have little influence on the relevant energy gaps, since the TiO_2 electronic states are delocalized over many atoms and the electron−phonon coupling in bulk TiO_2 is weak. Note that, in contrast to the bulk modes, the surface hydroxyl groups can play an important role in the ET. Our earlier studies of the electron injection[68] showed that the hydroxyl modes modulate the localization of the PE state and therefore change the electron donor−acceptor coupling.

When considering the ET between the electrolyte mediator and the chromophore, one wonders whether the low-frequency I_2^- modes or the high frequency alizarin vibrations are more important. Interestingly, the HOMO(I_2^-)−HOMO-1(alizarin) energy gap in the alizarin/I_2^-/TiO_2 system is much more strongly modulated by the slow I_2^- vibrations (bottom panel of Figure 7). The alizarin peaks are visible, but they are very small. The electronic state localization argument applies here as well. The I_2^- state localized over only two atoms is much more sensitive to the interatomic distances than the alizarin state that spreads over 18 carbon and oxygen atoms (Figure 4).

Lower frequency motions of the chromophore molecule are generally more important than the high-frequency modes. The lower frequency modes induce larger scale changes in the geometric structure and, therefore, are able to affect the energies of the delocalized molecular orbitals more strongly. This

(98) Zanni, M. T.; Greenblatt, B. J; Neumark, D. M. *J. Chem. Phys.* **1998**, *109*, 9648.

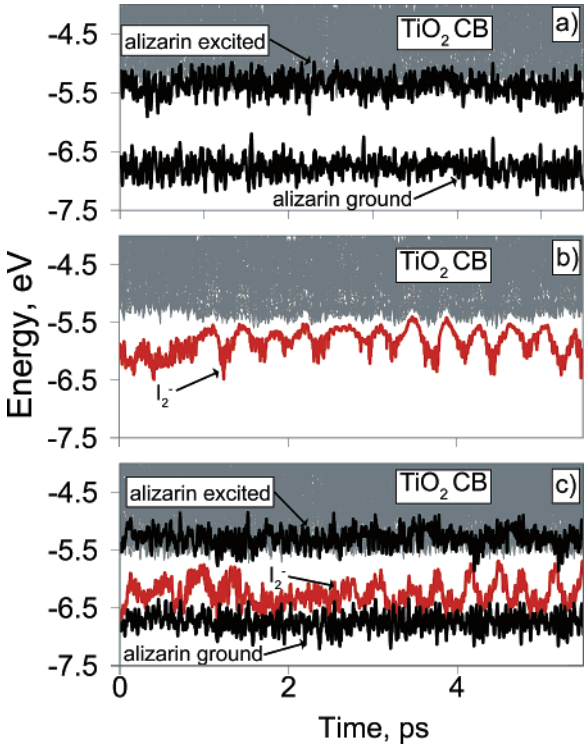

Figure 6. Evolution of the state energies in the alizarin/TiO_2, I_2^-/TiO_2, and alizarin/I_2^-/TiO_2 systems. Distortions in the optimal geometries, Figure 2, caused by thermal fluctuations have a significant effect on the state energies, compared to the corresponding values at zero temperature, Figure 3. The TiO_2 states are affected least, as expected for delocalized states in a large system. Both alizarin and I_2^- states exhibit significant energy fluctuations. The alizarin excited state often crosses into the TiO_2 CB, while the I_2^- state closely approaches the band.

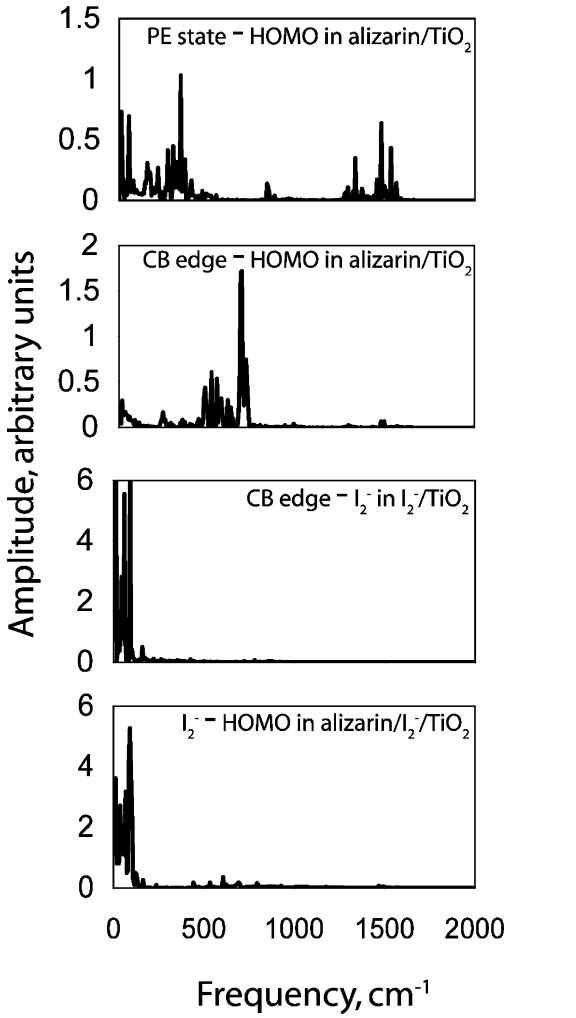

Figure 7. Fourier transforms of the autocorrelations of the following energy gaps, from top to bottom: PE state−HOMO(alizarin) in alizarin/TiO_2, CB edge−HOMO(alizarin) gap in alizarin/TiO_2, CB edge−HOMO(I_2^-) in I_2^-/TiO_2, and HOMO(I_2^-)−HOMO-1(alizarin) in alizarin/I_2^-/TiO_2. The frequencies identify the vibrations that facilitate the electron back-transfer. The back-transfer from TiO_2 to alizarin occurs by coupling to high- and low-frequency modes, while the back-transfer to I_2^- occurs by coupling only to low-frequency modes. Both types of modes are available during the transfer between alizarin and I_2^-, but the low-frequency modes of I_2^- dominate. The large amplitude seen with the I_2^- modes agrees with the substantial fluctuation of the I_2^- energies in parts (b) and (c) in Figure 6.

observation is true even for the PE state−HOMO(alizarin) gap that is primarily determined by the chromophore alone and, therefore, depends only on intramolecular vibrations, top panel of Figure 7. Additionally, intermolecular vibrations involving alizarin appear in the dynamics of the electron injection,[68] recombination, and transfer from the electrolyte to the chromophore. Figure 8 shows a bending mode of alizarin with respect to the TiO_2 surface in the combined system. This substantial movement of the chromophore has the potential to significantly change the nature of the alizarin/TiO_2 and alizarin/I_2^- interactions, again showing the need to include dynamics in the characterization of a system's properties.

3.5. Electronic Relaxation Inside the TiO_2 CB. Following the photoinduced electron injection from a chromophore to the TiO_2 CB, which we studied in our previous work,[65−72] the injected electron relaxes to the bottom of the CB. This process is detailed in Figure 9, using the I_2^-/TiO_2 simulation cell (Figure 2) and restricting the electron dynamics to the TiO_2 CB states. While in the alizarin/TiO_2 system the electron injection occurs near the bottom of the CB, and the intraband electron relaxation is not needed; in the majority of dye-sensitized semiconductor systems the electron is injected well inside the CB. Part (a) of Figure 9 shows the DOS of the TiO_2 CB, with the arrows indicating the four different electron injection energies considered in the present study. The blue arrow 4 corresponds to the band edge where alizarin typically injects, while the other three arrows represent hypothetical chromophores injecting around the DOS local maxima. The insert in Figure 9a gives the hopping probability distribution as a function of the energy difference between the initial and final states. The data shows that many hops induce small energy changes; some hops occur upward in energy, and large negative hops make a strong contribution to the energy relaxation.

Figure 9b shows the population of the CB edge as a function of time for the different injection energies that are shown in part (a). The data indicate that the movement of charge to the band edge happens at approximately the same rate regardless of the position of the PE state. This supports the idea that transfers between energetically separated states make a contribution to the movement of the electron downward through the band; otherwise the HOMO population rise would be faster for PE states low in the band (green 3) than for those high in the band (black 1). The fast transfer from the upper regions of the DOS to the band edge is due to the fact that there are states throughout the CB that have large spatial overlaps with the band edge states. Because the DOS is larger at higher energies, the transfer between the high energy states is fast, and one of the

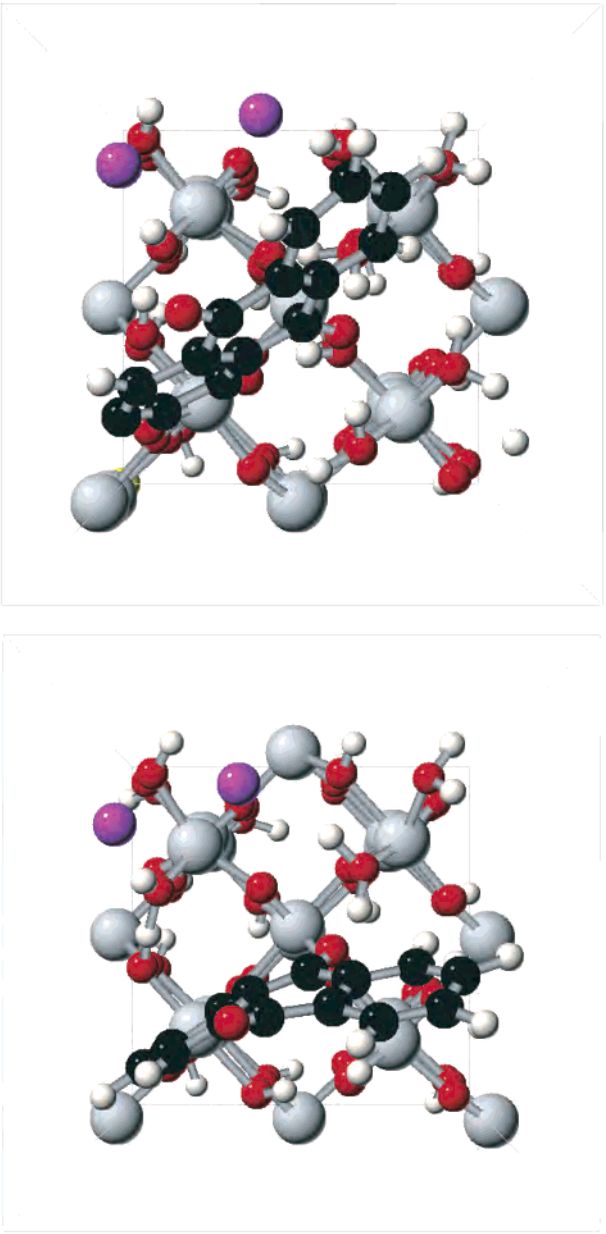

Figure 8. Two different positions of alizarin in the alizarin/I_2^-/TiO_2 system illustrating the extent of the thermally induced fluctuations modulating the electronic state energies, Figure 6. The atoms are denoted the same as those in Figure 2.

states with strong coupling to the band edge is usually populated quite quickly. Since there are a number of states close to each other in energy at the bottom of the band, the relaxation creates a quasi-equilibrium set of populations of these states, corresponding to room temperature. This quasi-equilibrium is responsible for the large fluctuations in the band edge population that persist after 300 fs. Larger numbers of initial conditions and SH trajectories lead to better averaging and smoother band edge populations. In the presence of electron harvesters, such as a chromophore or an electrolyte, the electron can relax further, and the population of the band edge state will decrease. This process is considered in the later sections.

The movement of the electron immediately after injection is detailed in part (c) of Figure 9. Shown are the evolution of the populations of the PE state and its nearest neighbors up (+1) and down (−1, −2) in energy. As represented by the simulation cell, these states are separated from each other by about 10 meV. As the PE state occupation decreases, the occupation of the state below it, PE state-1, increases; the occupation of the state above it, PE state+1, increases as well, but not as much due to the Boltzmann factor. The population of the state that is two states below, PE state-2, also increases. It reaches a maximum after PE state-1, indicating that some transfer to PE state-2 occurs through PE state-1. But since its maximum is much smaller, almost by a factor of 2, there is substantial transfer from PE state-1 to lower states that bypasses PE state-2. It is possible that the transfer from PE state-2 to PE state-3 is faster than the transfer from PE state-1 to PE state-2, and that is why the maximum is smaller, but this pattern of smaller occupation bumps is seen for each successive state; this is additional strong evidence for the importance of transfers between energetically separated states.

Interestingly, the CB edge state population increases faster than the CB edge+1 and CB edge+2 state populations (Figure 9d). This suggests that a fraction of the electrons are transferring to the edge state and then moving upward in energy to the neighboring states.

3.6. Electron Recombination with Electrolyte. The presence of the I_2^- species does not significantly affect the initial stages of the electron relaxation inside the TiO_2 CB (cf. Figures 9 and 10). The DOS of the combined I_2^-/TiO_2 system shown in part (a) of Figure 10 contains a new component originating from the I_2^- state (see also Figures 3 and 6), but only at low energies. The transfer of the electron between the band states directly after injection from the PE state is almost exactly the same (Figure 10c) which is to be expected, since the two simulations differ only in the presence of the I_2^- state below the band edge. A minor difference during the initial time period is seen in the population of the lowest energy states in each system. The CB edge in the system with no I_2^- is populated at a slightly faster rate than the population rate of the I_2^- state in the other system. There is no obvious relationship between the rate increase of the population of the I_2^- state (Figure 10b) and the position of the PE state in the CB (Figure 10a). In each case it is populated by an exponential time constant of approximately 190 fs.

The longer time dynamics with and without I_2^- differ significantly however (Figure 10d) since the electron leaves the CB and transfers onto the electrolyte mediator. The CB edge state is populated only transiently. The buildup of the electron density at the CB edge is appreciable, about 20% (this is due to the fact that the transition from the edge state to the I_2^- state is not as fast as the transitions between the neighboring semiconductor states), but this buildup is short-lived. Eventually the electron moves to the I_2^- state, which is far enough below the CB that the Boltzmann factor makes upward transitions very unlikely. This is why the I_2^- state population approaches 1, part (b), and the edge populations decrease to 0, part (d). Note that the I_2^- population rises substantially even before the CB edge state reaches its maximum, part (d). This is because there are transitions from states higher in the CB directly to the I_2^- state.

As discussed above, the energy differences between the KS orbitals in the DFT calculations seriously underestimate the size of the gaps between the states. In particular, the experimental[6] redox potential of the I^-/I_3^- mediator is 0.5 eV lower relative to the TiO_2 CB than the gap between the TiO_2 band edge and I_2^- orbitals reported in Figure 3. In order to test the significance

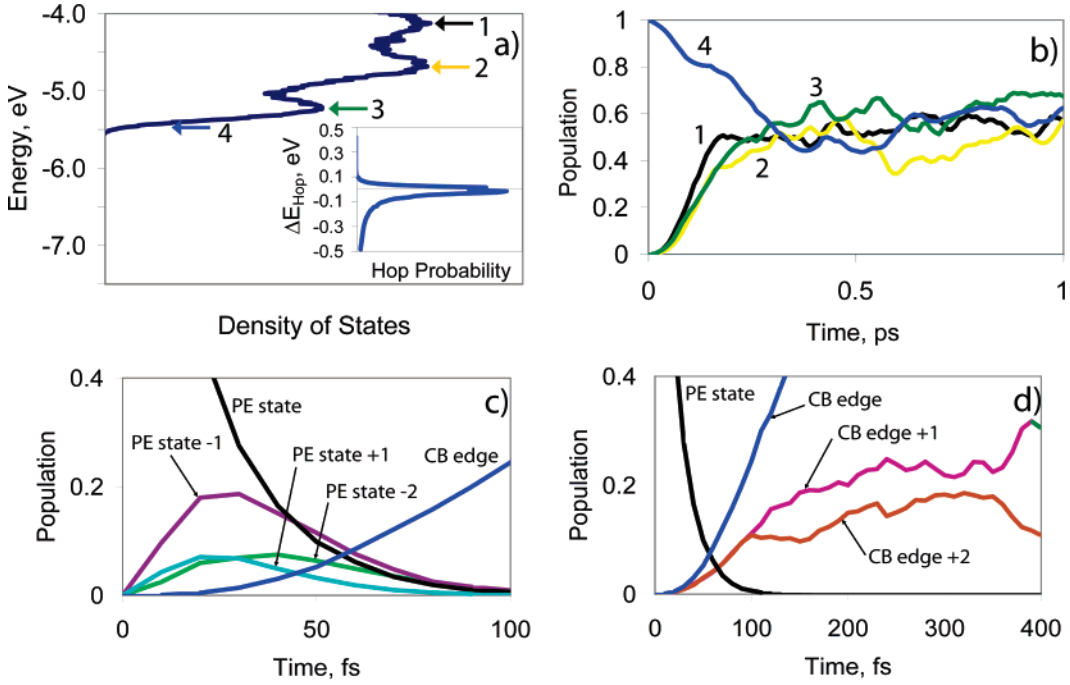

Figure 9. Electron relaxation in the TiO_2 CB following electron injection at different energies; see Figure 1. (a) Density of states for the CB; the arrows mark the electron injection energies; the insert plots hopping probability as a function of hop energy. Hops down in energy are more probable than hops up in energy, causing overall energy relaxation. (b) Dynamics of the population of the lowest energy CB state for different injection energies, specified by the arrows in part (a). Line 4 describes the situation, in which the electron is injected to the CB state. Nearly independent of the injection energy, electrons reach the band edge within 100 fs and are distributed among several band edge states with Boltzmann probabilities. (c and d) Short and long time dynamics of the populations of states near the photoexcited (PE) and CB edge states after the high energy injection described by arrow 1 in part (a). The injected electron spreads over many states, relaxes down in energy, and eventually localizes at the CB edge.

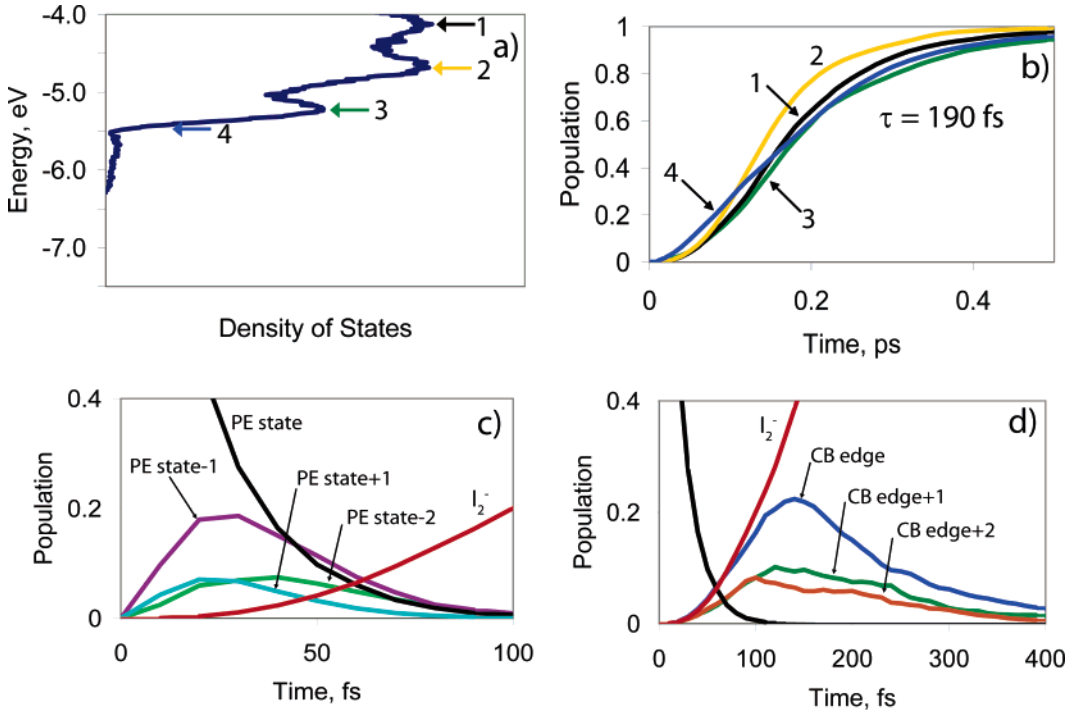

Figure 10. Electron relaxation in the I_2^-/TiO_2 system. (a−d) Analogous to the corresponding parts in Figure 9. The differences arise due to the presence of the I_2^- state located inside the TiO_2 band gap; see Figures 3 and 6. Notice the extra density of states in part (a) below −5.5 eV. The I_2^- state is populated by 90% or more within 0.5 ps independent of the injection energy. The time constant shown in part (b) is derived from the exponential fit of the data.

of the discrepancy between the experimental and theoretical energy gaps, we shifted the I_2^- state energy down by 0.5 eV in the I_2^-/TiO_2 system and repeated the calculations. In this case, the repopulation of the I_2^- state time scale increased from 190 to 230 fs and none of the above conclusions changed. Either result indicates that the electrolyte can efficiently scavenger the photoinjected electron, provided that both the electron and the electrolyte mediator approach each other near the TiO_2 surface.

3.7. Back-ET to the Dye. The rate of the back-ET from the TiO_2 surface to the alizarin chromophore is reported in Figure

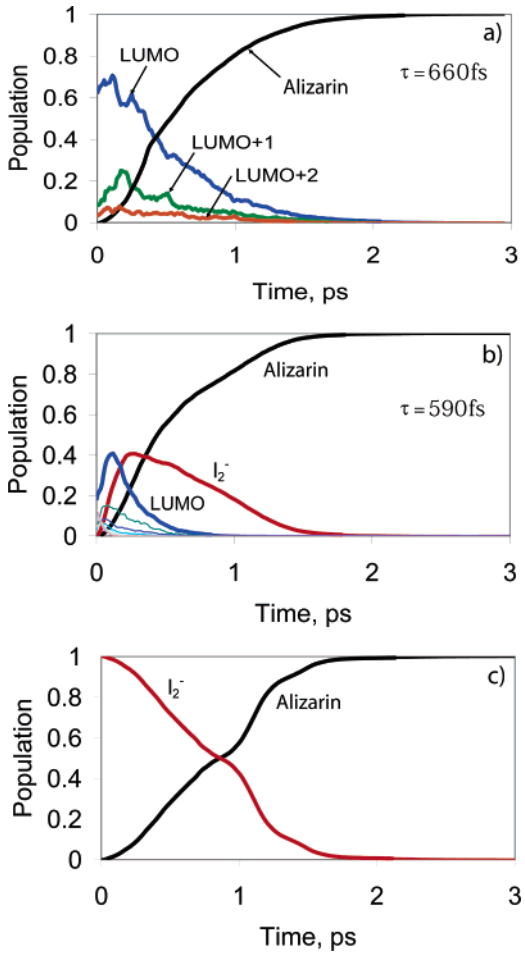

Figure 11. Electron relaxation in the alizarin systems. (a) Population dynamics of the photoexcited electron in the alizarin/TiO_2 system. Initially, the electron occupies the alizarin excited state, which is the system's LUMO 70% of the time, the system's LUMO+1 10% of the time, etc.; see Figure 6. The electron relaxes to the alizarin ground state on the 660 fs time scale, as determined by the exponential fit of the alizarin ground state population. (b) Population dynamics of the photoexcited electron in the alizarin/I_2^-/TiO_2 system. As in part (a), the electron occupies the alizarin excited state at time zero. The I_2^- state is energetically between the alizarin ground state and the TiO_2 CB (see Figures 3 and 6) and actively participates in the relaxation. The electron reaches the alizarin ground state on the 590 fs time scale, slightly faster than in the absence of I_2^-. (c) Regeneration of the neutral dye by electron transfer from the I_2^- redox mediator to alizarin. The rate of the dye regeneration is strongly dependent on the dye$-I_2^-$ distance, which is not fixed by chemical binding, and is generally smaller than the rate of the back-transfer of the electron trapped at the TiO_2 surface to alizarin, parts (a) and (b). The distance dependence is evident in the stepwise character of the transfer, which accelerates when I_2^- approaches the dye.

11a, which plots the time-dependent populations of the alizarin HOMO and three unoccupied orbitals above it, calculated for the alizarin/TiO_2 system (Figure 2). Following the photoexcitation and the ultrafast injection that were studied in our earlier work,[67−72] the electron returns to the chromophore on a significantly slower time scale. The initial populations of the LUMO, LUMO+1, and LUMO+2 are determined by the location of the PE state relative to the CB edge. Since the PE state is often below the CB edge and therefore is the LUMO, the LUMO population is about 60% at the beginning of the dynamics run. The portion of the electron that is in higher states moves down to the edge states in approximately 100 fs; this can be seen in the slight initial increase in the populations of the edge states.

The value of the time constant for back-ET depends on whether the orbital energy gap (Figure 3) or the experimental value[52] is used for the alizarin photoexcitation energy. The 660 fs time reported in Figure 11a is obtained using the orbital energies. Repeating the NA dynamics with the gap scaled to the experimental value gives 1100 fs. The difference is substantial; it falls, however, well within the range of the experimental values[30,33,43,45,49−55] The back-ET to the chromophore is substantially slower than the transfer from the CB to the electrolyte (Figure 10) indicating that if the electrolyte mediator is able to approach the surface, it becomes a more efficient electron acceptor than the chromophore.

3.8. Electron Relaxation in the Presence of Both Chromophore and Electrolyte. In the combined system (Figure 11b) the electron can leave TiO_2 by going either to the chromophore or to the electrolyte mediator. Since the PE state extends further into the band in the combined system than it does in the system with just alizarin, part (a), the initial occupation of the LUMO is substantially lower, around 20%. The electron dynamics involve multiple components, the fastest of which represents electron relaxation to the LUMO, which is the bottom of the CB. Simultaneously with the relaxation inside the band, the electron starts transferring to I_2^- and then to alizarin. The maximum values of the transient occupations of the CB edge (LUMO) and I_2^- are around 40%. The time constant for populating the alizarin ground state is 590 fs, which is on the same order as the corresponding time constant in the absence of I_2^- (Figure 11a). It is important to realize that a large amount of the transfer to the alizarin ground state, 33%, derives directly from states in the CB and, therefore, bypasses the I_2^- state entirely. As with the alizarin/TiO_2 system, scaling the energy levels to the experimental values slows down the back-ET. The transient occupations of the LUMO and I_2^- states reach higher values. However, the overall qualitative picture of the electron relaxation remains the same.

An additional complication in the combined system arises because the I_2^- orbital that is above the alizarin ground state is already occupied by an electron before the photoexcitation. Therefore, as soon as the PE electron leaves the dye on the 6 fs time scale,[53,67,68] the I_2^- electron can transfer to the dye; it cannot move up to the TiO_2 because of the large energy gap between the I_2^- state and the TiO_2 CB (Figures 3 and 6). When the excited alizarin state in the combined system is the PE state, the transfer to I_2^- is on the same order as the rate of transfer from I_2^- to the alizarin HOMO. The presence of the extra mediator electron, therefore, increases the rate of overall back-ET to the chromophore. When the I_2^- state in the combined system is the initial state of the simulation, however, the rate of transfer to the alizarin HOMO is significantly slower (see Figure 11c analyzed below). We believe that this slower rate represents the actual rate of transfer between the mediator and the chromophore ground state, in which case the PE electron reaches I_2^- faster than an electron from I_2^- moves to the chromophore, and the presence of the extra electron in the I_2^- state cannot change the overall sequence of electron relaxation events.

The reason why the transfer rate between two states is dependent on the initial state of the simulation is rooted in the FSSH procedure. In his 1990 paper on FSSH, Tully suggested that the coefficients that are used to determine the probability

of a hop, eq 8, should be integrated continuously to retain electronic quantum coherence effects;[80] they are not reset after a hop between states. In our simulations this leads to the following: when the electron is initially placed in the excited alizarin state and the electron density is evolved, the coefficients associated with the I_2^- state and the alizarin HOMO increase relatively quickly. This rapid increase is due to the fact that the PE state is usually spread across both the chromophore and the semiconductor surface and, therefore, has a relatively strong coupling to both the alizarin HOMO and the I_2^- state, which is slightly delocalized onto the TiO_2. By the time an electron has hopped to the mediator, the coefficient a_{kj} in eq 9, where k is the alizarin HOMO and j is the I_2^- state, is large enough that the probability of a hop between the states is large. The situation is very different when the electron is initially placed in the I_2^- state and the electron density is evolved. In this case the coefficient corresponding to the alizarin HOMO state rises much more slowly, because the coupling between the alizarin HOMO and the I_2^- state is so small. This means that the probability of transfer between the I_2^- state and the alizarin HOMO remains small throughout the SH trajectory, and the ET is slow.

Periodically resetting the coefficients after hops take place would cause the probability of a hop to be independent of the initial state of the simulation. In the system with the mediator, this would cause the transfer from the PE state to the alizarin HOMO to be slightly slower, because the transfer through the I_2^- state would take longer. The effects of quantum decoherence[87−89] on the ET processes at the chromophore−semiconductor interface require further investigation. We expect that back-ET will be slightly slowed down by the loss of quantum coherence.

3.9. ET from the Electrolyte to the Dye. In a solar cell, the positive charge created in the chromophore by the photoexcitation and interfacial electron injection is quenched by the negative charge that is brought in by the redox mediator. The two species carry opposite charges and are therefore electrically attracted. Since the chromophore is chemically attached to the semiconductor surface, the electrolyte−chromophore interaction occurs at the surface, as represented by the alizarin/I_2^-/TiO_2 simulation cell (Figure 2). Figure 11c considers the dynamics of this ET process. An electron placed in the I_2^- state moves down in energy to the alizarin state relatively slowly. It may seem surprising that this transfer is so slow, since the two states are closer in energy than, for instance, the TiO_2 CB and alizarin states, between which the relaxation is faster (see parts (a) and (b) in Figure 11). The reason is that the rate of the ET between I_2^- and alizarin is determined by the electron donor−acceptor coupling, which must be substantially weaker for the spatially separated molecules than for the alizarin−TiO_2 surface donor−acceptor pair, which is chemically bound. Indeed, the nonexponential rise of the occupation of the alizarin ground state that can be seen in Figure 11c indicates that the ET strongly depends on the chromophore−mediator distance. The step in the state occupations seen in the figure is due to the change in the relative positions of the donor and acceptor species, involving notable fluctuations of the location of the I_2^- and the slow frequency wagging motion of alizarin relative to the surface (Figure 8). The electron coupling between alizarin and I_2^- may occur not only through space but also through bonds involving the TiO_2 surface, as indicated by delocalization of both alizarin and, to a lesser extent, I_2^- states onto the surface, Figures 4 (top panel) and 5. Further evidence supporting the through-bond contribution to the electrolyte−chromophore ET is provided by the increased delocalization of the I_2^- state onto the surface in the combined system; cf. the lower and upper panels of Figure 5.

4. Conclusions

In this paper we have analyzed the electron dynamics at the alizarin−TiO_2 interface separately and in the presence of an electrolyte mediator. The system represents the interface in a Grätzel type solar cell and is also a good general model for studying the electron dynamics in systems with molecular/bulk components. We described the electron injection from the molecule to the semiconductor in an earlier paper;[68] here we have concentrated on the dynamics that occur after the initial transfer, including the relaxation of the injected electron inside the TiO_2 CB, recombination of the injected electron with the chromophore−cation, electron loss from the semiconductor to an electrolyte mediator, and regeneration of the neutral chromophore by ET from the mediator. The relaxation inside the CB is a source of voltage loss in the solar cell. The transfer back to the dye cation and to the electrolyte is particularly important, as it represents a short circuit in the Grätzel cell that leads to a loss of current.

By including dynamics in the simulations, we have been able to demonstrate the differences between the geometric and electronic structure of the system at 0 K and at ambient temperature. Having characterized the electronic properties of the interface in its optimal geometry, we have detailed the vibrational modes that contribute to the ET processes, all of which proceed by strong coupling to vibrations via the NA mechanism. Thermally activated atomic motions not only affect the system geometry, in one case resulting in a dissociation of an adsorbed species, but also greatly change the electronic properties, such as donor−acceptor coupling, state energies, and localizations. A rich and sometimes unexpected interplay between the electronic and vibrational dynamics has been observed.

We have simulated the NA MD in real time and at the atomistic level using a mixed quantum-classical approach that combines TD DFT with SH in the KS representation. This method, unlike the Ehrenfest and classical path techniques used previously, maintains detailed balance and allows us to model electron relaxation. The simulation carried out for the entire system that contains many electronic states have shown that the relaxation to the edge of the CB occurs on an ultrafast time scale, with the rate independent of the energy of the injected electron relative to the CB edge. This occurs because, as electrons progress down the band, they populate states that have strong coupling with band edge states. Large downward hops in energy between these states and the band edge states make a significant contribution to the dynamics.

The electron loss to the chromophore and the electrolyte mediator has been investigated under the assumption that the electron is already trapped near the surface. Our earlier simulations have shown that the injected electron rapidly delocalizes into the bulk. Nevertheless, in the presence of trap states the electron is less likely to leave the surface, and it can always return due to its attraction to the chromophore−cation, the electrolyte, or simply because of the large surface area of

the dye-sensitized semiconductor. We have found that the back transfer of the electron trapped near the surface to the electrolyte can occur on a picosecond time scale, regardless of the electron injection energy. This assumes that the mediator can closely approach the surface, which is reasonable since the electrolyte is attracted to the oxidized chromophore and must remain near the surface in order to reduce the chromophore. Our simulations that model the back-ET from the semiconductor to the chromophore have shown that this transfer occurs on a picosecond or longer time scale, in agreement with the experimental values.[30,33,43,45,49−55] We also showed that, in the presence of the electrolyte mediator, the back transfer from the semiconductor to the dye occurs on a similar time scale. Even with the presence of the mediator close to the dye and the surface, the electron often transfers directly from the CB edge back to the dye.

We have shown that an electrolyte molecule can approach the surface near the attached chromophore and then transfer an electron onto the chromophore, preparing it for the next photovoltaic cycle. The simulation results indicate that the electrolyte−chromophore coupling can occur both through space and with the help of the surface states. Once the electrolyte species passes its charge to the dye, it is no longer strongly attracted to the surface and will diffuse away.

The unique perspective provided by the atomistic simulation indicates that the rates and mechanisms of the interfacial ET processes depend on the molecular structure of the chromophore and the bridge connecting the chromophore to the surface. If the bridge is short, as in the case of alizarin and catechol, the chromophore−semiconductor coupling is strong and the electron injection proceeds by the adiabatic mechanism.[67,68,70] The back-ET is also fast; however, it necessarily proceeds by the NA mechanism, since the energy gap between the bottom of the TiO_2 CB and the chromophore ground state is large. The high back-ET rate seen in the alizarin system is due to strong NA coupling. The latter depends on both the overlap between the initial and final electronic states and the velocity of the vibrational motions, see eq 7.

The dependence of the NA coupling on the electronic overlap suggests that back-ET can be reduced by choosing chromophores with ground states localized away from the surface. Alizarin in particular presents a poor choice from this point of view, since its ground state (top panel of Figure 4) is localized toward the surface. Additional electron withdrawing groups to the other end of the molecule can be expected to shift the ground state electron density and reduce back-ET. The return of the electron to alizarin is rapid also because it is facilitated by relatively fast vibrational modes (top panel of Figure 7). The frequency of the vibrational modes that couple electronic states is generally lower in chromophores containing heavier atoms, especially if the electronic states are localized on those atoms, as well as in chromophores with more delocalized states, as in perylene.[37] Somewhat surprisingly, the rate of back-ET is not particularly sensitive to the exact value of the energy gap between the TiO_2 CB and the chromophore ground state, as long as the gap remains large.

Transition-metal-based chromophores that are most commonly used in Grätzel cells take advantage of the dependence of the NA coupling on both the electronic overlap and the vibrational velocity. In such chromophores the ground state is localized away from the surface and on the transition metal. The latter is a heavy element, and therefore, the frequency of the vibrational motions that couple the ground state localized on the transition metal is low.

Longer bridges will slow down both electron injection and recombination. Due to the decrease of the chromophore−semiconductor coupling, the mechanism of the injection will change from adiabatic to NA, as seen already when the hydroxylic group is replaced with the carboxylic group.[65,66] Even though longer bridges slow down back-ET and, therefore current loss, efficient injection by the NA mechanism requires a high density of acceptor states. As a result, the injection must occur relatively high inside the TiO_2 CB, such that the ensueing relaxation inside the band will result in voltage loss.

As we pointed out earlier,[67] electron injection from alizarin into the edge of the CB can be used to decrease loss of energy and voltage in the Grätzel cell. At the same time, back-ET and current loss are increased. Our simulations show, however, that an electron injected into a defectless TiO_2 surface delocalizes into the bulk significantly faster than it transfers back onto alizarin. Surface defects and unsaturated dangling bonds present the real problem, since they will trap the injected electron, allowing back-ET to occur. Surface annealing as well as the reduction of the NA coupling by proper choice of the chromophore properties as discussed above can be used to reduce back-ET, while minimizing energy relaxation losses.

The results reported here and in our earlier publications[67,68,70] agree quantitatively with the available experimental data[52−54] and create a complete, real-time, atomistic picture of the electron dynamics at the alizarin−TiO_2 interface.

Acknowledgment. The authors are grateful to Michael Grätzel, Tim Lian, and Frank Willig for many fruitful discussions. The research was supported by DOE Award DE-FG02-05ER15755.

Supporting Information Available: The Supporting Information contains the complete author list for ref 92. This material is available free of charge via the Internet at http://pubs.acs.org.

JA0707198